

Achievable Rate Region of the Zero-Forcing Precoder in a 2×2 MU-MISO Broadcast VLC Channel with Per-LED Peak Power Constraint and Dimming Control

Amit Agarwal and Saif Khan Mohammed

Abstract—In this paper, we consider the 2×2 multi-user multiple-input-single-output (MU-MISO) broadcast visible light communication (VLC) channel with two light emitting diodes (LEDs) at the transmitter and a single photo diode (PD) at each of the two users. We propose an achievable rate region of the Zero-Forcing (ZF) precoder in this 2×2 MU-MISO VLC channel under a per-LED peak and average power constraint, where the average optical power emitted from each LED is fixed for constant lighting, but is controllable (referred to as dimming control in IEEE 802.15.7 standard on VLC). We analytically characterize the proposed rate region boundary and show that it is Pareto-optimal. Further analysis reveals that the largest rate region is achieved when the fixed per-LED average optical power is half of the allowed per-LED peak optical power. We also propose a novel transceiver architecture where the channel encoder and dimming control are separated which greatly simplifies the complexity of the transceiver. A case study of an indoor VLC channel with the proposed transceiver reveals that the achievable information rates are sensitive to the placement of the LEDs and the PDs. An interesting observation is that for a given placement of LEDs in a $5 \text{ m} \times 5 \text{ m} \times 3 \text{ m}$ room, even with a substantial displacement of the users from their optimum placement, reduction in the achievable rates is not significant. This observation could therefore be used to define “coverage zones” within a room where the reduction in the information rates to the two users is within an acceptable tolerance limit.

Index Terms—Visible light communication, rate region, zero-forcing, multi-user, multiple-input-multiple-output.

I. INTRODUCTION

Visible light communication (VLC) is a form of optical wireless communication (OWC) technology which can provide high speed indoor wireless data transmission using existing infrastructure for lighting. One distinctive advantage of VLC technology is that it utilizes the unused visible band of the electromagnetic spectrum and does not interfere with the existing radio frequency (RF) communication in the UHF (Ultra High Frequency) band [1], [2].

In VLC systems, it is common to use intensity modulation (IM) via light emitting diode (LEDs) for transmission of information signal and direct detection (DD) via photodiodes (PDs)

for the recovery of the information signal [1]. Contrary to RF systems, in VLC systems the modulation symbols must be non-negative and real valued as information is communicated by modulating the power/intensity of the light emitted by the optical source (LED). The modulation symbols are also constrained to be less than a pre-determined value as the intensity of the light emitted by the LED is peak constrained due to safety regulations and also due to the limited linear range of the transfer function of LEDs [1], [3]. Moreover, due to constant lighting the mean value of the modulation symbol is also fixed (i.e., non-time varying) and can be adjusted according to the users’ requirement (dimming target) [4], [5].

Due to these constraints, analysis performed for RF systems is not directly applicable to VLC systems. For example, the capacity of the RF single-input-single-output (SISO) additive white Gaussian noise (AWGN) channel is well known and it has been shown that the *Gaussian* input distribution is capacity achieving. For the case of the optical wireless AWGN SISO channel with IM/DD transceiver, closed form expression for the capacity is still not known, though several inner and outer bounds have been proposed [6]–[8]. However, it has been shown that the capacity achieving input distribution for the IM/DD SISO AWGN optical wireless channel is discrete [9], and has been computed numerically in [10]. Similarly, for the case of dimmable VLC IM/DD SISO channel with peak constraint, there is no closed form expression for the capacity. However following a similar approach as in [6], an upper and lower bound is presented in [11].

Recently, there has been a lot of interest in multi-user multiple-input multiple-output/single-output (MU-MIMO/MISO) VLC systems, where multiple LEDs are used for information transmission to multiple non-cooperative PDs (users) [12], [1]. Such systems have been shown to enhance the system sum rate when compared to SISO VLC systems [13], [14].

In [13], the information sum rate of MU-MIMO VLC broadcast systems has been studied under the non-negativity constraint on the signal transmitted from each LED, and also a per-LED average transmitted power constraint with no dimming control. The block diagonalization precoder in [13] is used to suppress the multi-user interference and the numerically computed achievable sum rate is shown to be sensitive to the placement of the users and the rotation of the PDs. However, they do not consider peak power constraints

The authors are with the Department of Electrical Engineering, Indian Institute of Technology Delhi (IITD), New delhi, India. Saif Khan Mohammed is also associated with Bharti School of Telecommunication Technology and Management (BSTTM), IIT Delhi. Email: saifkhanmohammed@gmail.com. This work is supported by the Visvesvaraya Young Faculty Research Fellowship (YFRF) of the Ministry of Electronics and Information Technology, Govt. of India.

which is important due to eye safety regulations and also due to the requirement of limited interference to other VLC systems.

Per-LED peak and average power constraint has been considered in [14], where the sum-rate of the zero forcing (ZF) precoder is maximized in a IM/DD based MU-MIMO/MISO VLC systems. However, in many practical scenarios fairness is required and therefore maximizing the sum rate might not always be the desired operating regime. For example we would like to find the maximum possible rate such that each user gets the same rate. Such operating points can only be obtained from the rate region characterization of the MU-MIMO VLC systems. In [15], authors have proposed inner and outer bounds on the capacity region of a two user IM/DD broadcast VLC system where the transmitter has a single LED and each user has a single PD. Per-LED average and peak power constraints are considered. The authors have extended their work to more than two users in [16]. However, in both [15] and [16], the transmitter has *only one LED*. Furthermore, dimming control is not considered in [13]–[16].

The capacity/achievable rate region of a IM/DD based VLC broadcast channel where the transmitter has $N > 1$ LEDs and $M > 1$ users having one PD each, is still an open and challenging problem, primarily due to the non-negativity, peak and average constraints on the electrical signal input to each LED.

In this paper, we consider the smallest instance of this open problem along with dimming control, i.e., with $N = 2$ LEDs at the transmitter and $M = 2$ users (each having one PD). Dimming control is required in indoor VLC systems since the illumination should *not* vary with time on its own and should be controllable by the users. Therefore, in this paper, in addition to the peak and non-negativity constraints, we constrain the average optical power radiated by each LED to be fixed, i.e., non-time varying. Subsequently in this paper we refer to this system as the 2×2 MU-MISO VLC broadcast system.

The major contributions of this paper are as follows:

- 1) In Section III, we propose an achievable rate region for the 2×2 MU-MISO VLC broadcast system with the ZF precoder. In this section through analysis we show that the per-LED non-negativity and peak constraint restricts the information symbol vector for the two users (i.e., (u_1, u_2)) to lie within a parallelogram $R_{//}$. Each achievable rate pair (R_1, R_2) then corresponds to a rectangle which lies within $R_{//}$. The rate $R_i, i = 1, 2$ to the i^{th} user depends on the length of the rectangle along the u_i -axis. Due to the same average optical power constraint at each LED, these rectangles should also have their midpoint (i.e., point of intersection of the diagonals of the rectangle) at a fixed point on the diagonal of $R_{//}$ denoted by D.¹ This fixed point D on the diagonal of $R_{//}$ is non-time varying, but can be controlled by the user depending upon the illumination requirement. This feature of the proposed system enables

dimming control.

- 2) In Section III, We also mathematically define the proposed rate region of the ZF precoder for a fix dimming target.
- 3) In Section IV, we analytically characterize the boundary of the proposed rate region by deriving explicit expressions for the largest possible length along the u_2 -axis of some rectangle inside $R_{//}$ whose midpoint coincides with the fixed point D on the diagonal of $R_{//}$ and whose length along the u_1 -axis is given. *Through analysis we also show that the rate region boundary is Pareto-optimal.*
- 4) We also analyze the variation in the rate region with change in the dimming level. In depth analysis reveals that the largest rate region is achieved when the fixed point D lies at the midpoint of the diagonal of $R_{//}$, i.e., when the fixed per-LED average optical transmit power is half of the per-LED peak optical power.
- 5) For practical scenarios with fairness constraints, through analysis we show that the largest achievable rate pair (R_1, R_2) such that $R_2 = \alpha R_1$ is given by the unique intersection of the proposed rate region boundary with the straight line $R_2 = \alpha R_1$.
- 6) In Section V, from the point of view of practical implementation we also propose a novel transceiver architecture where the same channel encoder can be used irrespective of the level of dimming control.
- 7) Analytical results have been supported with numerical simulations in Section VI. It is observed that for a fixed placement of the two LEDs, the achievable information rates are a function of the placement of the two PDs/users. Specifically, we observe that for a given placement of the two LEDs, there exists an optimal placement of the two users which maximizes the symmetric rate. Another interesting observation is that in a $5 \text{ m} \times 5 \text{ m} \times 3 \text{ m}$ (height) room with the two LEDs attached to the ceiling and the two PDs placed in the horizontal plane at a height of 50 cm above the floor, even a user displacement of 60 cm from the optimal placement results in only approx. a 10 percent reduction in the symmetric rate when compared to the symmetric rate with the optimal placement of PDs². This allows for substantial mobility of the user terminals around their optimal placement which is specially desirable when the user terminals are mobile/portable. A practical application of the results derived in this paper could be in defining coverage zones for the PDs/users, i.e., the maximum allowable displacement of the users for a fixed desired upper limit on the percentage loss in the achievable information rates.

II. SYSTEM MODEL

We consider a 2×2 IM/DD MU-MISO VLC broadcast system. The transmitter of the MISO system is equipped with two LEDs and each user has a single photo-diode

¹Out of the two diagonals of $R_{//}$, we refer to the one which has one end point at the origin $(u_1, u_2) = (0,0)$.

²For this study the dimming control is such that the average optical power radiated from each LED is 30 percent of the peak allowed optical power

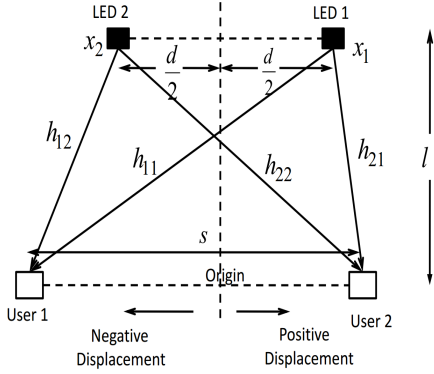


Fig. 1: 2×2 IM/DD MU-MISO VLC broadcast system.

(PD) (see Fig. 1).³ The LED converts the information carrying electrical signal to an intensity modulated optical signal and the PD at each user converts the received optical signal to electrical signal. The transmitter performs beamforming of the information symbols towards the two non-cooperative users. Let $u_1 \in \mathcal{U}_1$ and $u_2 \in \mathcal{U}_2$ be the information symbols intended for the first and second user respectively, where \mathcal{U}_1 and \mathcal{U}_2 are the information symbol alphabets for user 1 and user 2 respectively. Let x_i be the optical power transmitted from the i^{th} LED ($i = 1, 2$). At any time instance, the transmitted optical power vector $\mathbf{x} \triangleq [x_1 \ x_2]^T$ is given by

$$\mathbf{x} = \mathbf{A}\mathbf{u}, \quad (1)$$

where $\mathbf{u} \triangleq [u_1 \ u_2]^T$ and $\mathbf{A} \in \mathbb{R}^{2 \times 2}$ is the beamforming matrix. In this paper, we consider the following power constraints for our dimmable VLC system.

The instantaneous power transmitted from each LED is non negative and is less than some maximum limit P_0 due to skin and eye safety regulations [3]. Further, such a maximum limit on the transmitted power is required also due to limited interference requirement to the neighboring VLC systems, i.e.

$$0 \leq x_i \leq P_0, \quad i = 1, 2. \quad (2)$$

Since our VLC system is dimmable we further impose a per-LED average power constraint of the type

$$E[x_i] = \xi P_0, \quad i = 1, 2, \quad (3)$$

where $0 \leq \xi \leq 1$ is the dimming target [5]. For the sake of analysis, we define $x'_i \triangleq \frac{x_i}{P_0}$, $i = 1, 2$ as the normalized power transmitted from each LED. Consequently, the normalized optical power transmitted from each LED must satisfy the following constraints given by

$$0 \leq x'_i \leq 1 \quad \& \quad E[x'_i] = \xi, \quad i = 1, 2. \quad (4)$$

Assuming y_k , $k = 1, 2$ to be the normalized received electrical signal at the k^{th} user (after scaling down by P_0), the

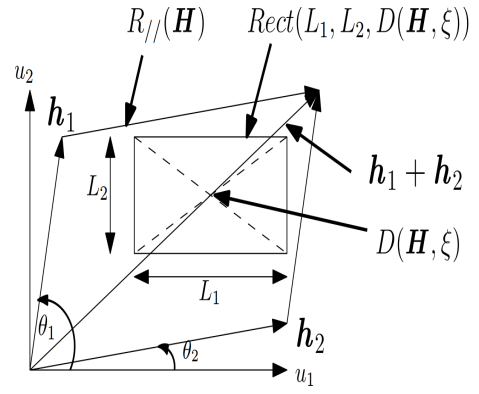


Fig. 2: The information vector \mathbf{u} is constrained to lie within the parallelogram $R_{//}(\mathbf{H})$ whose non-parallel sides are \mathbf{h}_1 and \mathbf{h}_2 . The rectangular region $\mathcal{U}_1 \times \mathcal{U}_2$ whose length along the u_1 axis is L_1 and that along the u_2 axis is L_2 and whose center lies at $D(\mathbf{H}, \xi)$ is denoted by $\text{Rect}(L_1, L_2, D(\mathbf{H}, \xi))$.

normalized received signal vector is given by⁴

$$\underbrace{\begin{bmatrix} y_1 \\ y_2 \end{bmatrix}}_{\triangleq \mathbf{y}} = \underbrace{\begin{bmatrix} h_{11} & h_{12} \\ h_{21} & h_{22} \end{bmatrix}}_{\triangleq \mathbf{H}} \underbrace{\begin{bmatrix} x'_1 \\ x'_2 \end{bmatrix}}_{\triangleq \mathbf{x}'} + \underbrace{\begin{bmatrix} n_1 \\ n_2 \end{bmatrix}}_{\triangleq \mathbf{n}},$$

$$\text{s.t. } 0 \leq x'_i \leq 1, \quad E[x'_i] = \xi, \quad i = 1, 2. \quad (5)$$

where $\mathbf{H} \triangleq [h_{ki}]_{2 \times 2}$ is the channel gain matrix. The channel gain coefficients between the i^{th} LED and the k^{th} user is denoted by h_{ki} , $i = 1, 2, k = 1, 2$.⁵ We further define $\mathbf{h}_1 \triangleq [h_{11} \ h_{21}]^T$ and $\mathbf{h}_2 \triangleq [h_{12} \ h_{22}]^T$ to be the channel vectors from LED 1 and LED 2 respectively. Further, n_1 and n_2 are the sum of the thermal noise and ambient light-induced shot noise at the respective users⁶ and are independent of x'_1 and x'_2 [12]. The noise signals are i.i.d. zero mean real AWGN with variance σ^2/P_0^2 , where σ^2 is the variance of the noise before the scaling down of the received signal by P_0 , i.e., $n \sim \mathcal{N}(0, (\sigma/P_0)^2)$.

III. AN ACHIEVABLE RATE REGION OF THE CHANNEL IN (5)

In this section, we derive an achievable rate region for the channel in (5) using the ZF precoder. For the 2×2 MU-MISO system discussed in section II, the ZF precoding matrix is uniquely given by $\mathbf{A} = P_0 \mathbf{H}^{-1}$, i.e., $\mathbf{x}' = \mathbf{x}/P_0 = \mathbf{A}\mathbf{u}/P_0 = P_0 \mathbf{H}^{-1} \mathbf{u}/P_0 = \mathbf{H}^{-1} \mathbf{u}$. Thus the received signal vector is given by

$$\mathbf{y} = \mathbf{H}\mathbf{x}' + \mathbf{n} = \mathbf{H}\mathbf{H}^{-1} \mathbf{u} + \mathbf{n} = \mathbf{u} + \mathbf{n}. \quad (6)$$

i.e., there is no multi-user interference (MUI). Since

$$\mathbf{u} = \mathbf{H}\mathbf{x}' = [\mathbf{h}_1 \ \mathbf{h}_2][x'_1 \ x'_2]^T, \quad (7)$$

⁴In subsequent discussions, by “received electrical signal”, we refer to the “normalized received electrical signal”.

⁵Note that h_{ki} 's are non negative and model the overall gains of the line of sight (LOS) optical path between the i^{th} LED and the k^{th} user and also the responsivity of the PD of the k^{th} user [3].

⁶Note that the above noise impairments of the received signal are the main impairments that are commonly assumed in VLC systems [3].

³Since each of the two users has a single PD we will be interchangeably using user and PD in subsequent discussions.

and $0 \leq x'_i \leq 1, i = 1, 2$ (see (4)) it follows that, the information signal vector \mathbf{u} must be limited to the region

$$R_{//}(\mathbf{H}) \triangleq \{\mathbf{u} \mid \mathbf{u} = \mathbf{H}\mathbf{x}', \quad 0 \leq x'_1 \leq 1, 0 \leq x'_2 \leq 1\}. \quad (8)$$

The region $R_{//}(\mathbf{H})$ is a parallelogram with its two non parallel sides as \mathbf{h}_1 and \mathbf{h}_2 (see $R_{//}(\mathbf{H})$ in Fig. 2). In addition to this, the diagonal of the parallelogram $R_{//}(\mathbf{H})$ is the vector $\mathbf{h}_1 + \mathbf{h}_2$ as shown in Fig. 2.

Let $E[\mathbf{u}] \triangleq [E[u_1] \ E[u_2]]^T$ be the mean information symbol vector. From (7) and (4), the mean information symbol vector is given by

$$E[\mathbf{u}] = \mathbf{H}E[\mathbf{x}'] = [\mathbf{h}_1 \ \mathbf{h}_2]E[x'_1 \ x'_2]^T \stackrel{(a)}{=} \xi(\mathbf{h}_1 + \mathbf{h}_2), \quad (9)$$

where step (a) follows from (5). Therefore, the mean information symbol pair $(E[u_1], E[u_2])$ is a point corresponding to the tip of the vector $E[\mathbf{u}] = \xi(\mathbf{h}_1 + \mathbf{h}_2)$. From (8) it is clear that the vector $(\mathbf{h}_1 + \mathbf{h}_2)$ is a diagonal of $R_{//}(\mathbf{H})$ (see Fig. 2). For a given $0 \leq \xi \leq 1$, the tip of the mean information symbol vector $\xi(\mathbf{h}_1 + \mathbf{h}_2)$ is therefore a *fixed* point on the diagonal $(\mathbf{h}_1 + \mathbf{h}_2)$. We denote this point by

$$D(\mathbf{H}, \xi) = (E[u_1], E[u_2]) \\ = (\xi(h_{11} + h_{12}), \xi(h_{21} + h_{22})). \quad (10)$$

With the ZF precoder, the broadcast channel in (5) is reduced to two parallel SISO (single-input single-output) optical channels between the transmitter and the two users (see (6)). Since $u_1 \in \mathcal{U}_1$ and $u_2 \in \mathcal{U}_2$ are independent and originate from different codebooks, it follows that $(u_1, u_2) \in \mathcal{U}_1 \times \mathcal{U}_2$. From (8), we know that (u_1, u_2) must belong to the parallelogram $R_{//}(\mathbf{H})$ and therefore

$$\mathcal{U}_1 \times \mathcal{U}_2 \subset R_{//}(\mathbf{H}). \quad (11)$$

In general we choose \mathcal{U}_1 and \mathcal{U}_2 to be intervals of the type $[a, b]$ [9]. Let the length of the intervals \mathcal{U}_1 and \mathcal{U}_2 be L_1 and L_2 respectively, i.e. $|\mathcal{U}_1| = L_1, |\mathcal{U}_2| = L_2$. With \mathcal{U}_1 and \mathcal{U}_2 as intervals, it is clear that $\mathcal{U}_1 \times \mathcal{U}_2$ must be a rectangle whose length along the u_1 axis is L_1 and that along the u_2 axis is L_2 . In this paper we assume u_1 and u_2 , to be *uniformly distributed* in the interval \mathcal{U}_1 and \mathcal{U}_2 respectively.⁷ Therefore, for a given \mathcal{U}_1 and \mathcal{U}_2 , the mean information symbol pair $(E[u_1], E[u_2])$ will lie at the point of intersection of the two diagonal of the rectangle $\mathcal{U}_1 \times \mathcal{U}_2$. We will subsequently call this point of intersection as the ‘‘midpoint’’ of the rectangle $\mathcal{U}_1 \times \mathcal{U}_2$ and will denote it by $\mathcal{C}(\mathcal{U}_1, \mathcal{U}_2)$.

From (10), it follows that the mean information symbol pair must exactly coincide with $D(\mathbf{H}, \xi)$, i.e.

$$\mathcal{C}(\mathcal{U}_1, \mathcal{U}_2) = D(\mathbf{H}, \xi) \quad (12)$$

The ZF precoder transforms the broadcast channel into two parallel SISO channels $y_i = u_i + n_i, u_i \in \mathcal{U}_i, i = 1, 2$. Let R_1 and R_2 denote the information rates achieved on these SISO channels with u_i distributed uniformly in \mathcal{U}_i . Any given \mathcal{U}_1 and \mathcal{U}_2 satisfying the conditions in (11) and (12) would satisfy the optical power constraints in (4) and would therefore

correspond to an achievable rate pair for the broadcast channel in (5). Since a rectangle in the $u_1 - u_2$ plane corresponds to a unique \mathcal{U}_1 and \mathcal{U}_2 and vice versa, it follows that any rectangle lying inside the parallelogram $R_{//}(\mathbf{H})$ and having its midpoint at $D(\mathbf{H}, \xi)$ will correspond to an achievable rate pair. In this paper, for the broadcast channel in (5), we therefore propose an achievable rate region which consists of rate pairs corresponding to such rectangles (one such rectangle is shown in Fig. 2). We define our proposed rate region more precisely in the following. Towards this end, we first formally define the achievable rate of a SISO AWGN optical channel, where the transmitted information symbol is constrained to lie in an interval.

Result 1. [From [6], [10]] *The achievable information rate of a SISO channel $y = u + n$ (where $u \sim \text{Unif}[a, b]$ and $n \sim \mathcal{N}(0, (\sigma/P_0)^2)$) depends on the interval $[a, b]$ only through its length $L = |b - a|$, and is given by the function*

$$C(L = |b - a|, P_0/\sigma) \triangleq I(u; y), \quad (13)$$

here $\text{Unif}[a, b]$ denote the uniform distribution in the interval $[a, b]$ and $I(u; y)$ is the mutual information between u and y .

Result 2. [From [6], [10]] *The function $C(L, P_0/\sigma)$ is continuous with respect to L and increases monotonically with increasing L for a fixed P_0/σ .*

Let $\text{Rect}(L_1, L_2, D(\mathbf{H}, \xi))$ denote the unique rectangle having its midpoint as $D(\mathbf{H}, \xi)$ and whose length along the u_1 axis is L_1 and that along the u_2 axis is L_2 (see Fig. 2). Any such rectangle $\text{Rect}(L_1, L_2, D(\mathbf{H}, \xi)) \subset R_{//}(\mathbf{H})$ will correspond to an achievable rate pair given by

$$(R_1, R_2) \triangleq (C(L_1, P_0/\sigma), C(L_2, P_0/\sigma)) \quad (14)$$

For a given $(\mathbf{H}, P_0/\sigma, \xi)$ the proposed achievable rate region for the ZF precoder is given by

$$R_{ZF}(\mathbf{H}, P_0/\sigma, \xi) \triangleq \bigcup_{(L_1, L_2) \in (L_1, L_2) \in S} \{C(L_1, P_0/\sigma), C(L_2, P_0/\sigma)\}, \quad (15)$$

where $S \triangleq \{(L_1 \geq 0, L_2 \geq 0) \mid \exists \text{Rect}(L_1, L_2, D(\mathbf{H}, \xi)) \subset R_{//}(\mathbf{H})\}$.

IV. CHARACTERIZING THE BOUNDARY OF THE RATE REGION $R_{ZF}(\mathbf{H}, P_0/\sigma, \xi)$

In this section, we completely characterize the boundary of the rate region, $R_{ZF}(\mathbf{H}, P_0/\sigma, \xi)$, for a fixed $(\mathbf{H}, P_0/\sigma, \xi)$. Towards this end, for each information rate R_1 achievable by the first user, we find the corresponding maximum possible information rate R_2 achievable by the second user. *Each pair of R_1 and its corresponding maximum possible R_2 is therefore a point on the boundary of the proposed rate region.* By increasing R_1 from 0 to its maximum possible value, all such (R_1, R_2) pairs characterize the boundary of the rate region.

From (15), we know that any achievable rate pair (R_1, R_2) in the proposed rate region $R_{ZF}(\mathbf{H}, P_0/\sigma, \xi)$ corresponds to some rectangle $\text{Rect}(L_1, L_2, D(\mathbf{H}, \xi))$. The rate to the i^{th} user, i.e. $R_i = C(L_i, P_0/\sigma), i = 1, 2$ depends only on the length of this rectangle along the u_i -axis. Since the

⁷At high SNR ($P_0/\sigma \gg 1$), uniformly distributed information symbol is near capacity achieving [10].

$C(L, P_0/\sigma)$ function is monotonic and continuous in its first argument, each value of R_i corresponds to a unique L_i and vice versa. Therefore, towards characterizing the boundary of $R_{ZF}(\mathbf{H}, P_0/\sigma, \xi)$, we note that for a given R_1 , i.e., for a given length L_1 along the u_1 -axis, we would like to find the largest possible R_2 , i.e., the largest possible L_2 such that the rectangle $Rect(L_1, L_2, D(\mathbf{H}, \xi))$ lies entirely inside $R_{//}(\mathbf{H})$. Hence, we can characterize the boundary of $R_{ZF}(\mathbf{H}, P_0/\sigma, \xi)$ simply by varying $L_1 = x$ from 0 to its maximum possible value (denoted by $L_1^{\max}(\xi)$), and for each value of $L_1 = x \in [0, L_1^{\max}(\xi)]$ we find the largest possible $L_2 = L_2^\xi(x)$ which gives us a corresponding rate pair $(R_1, R_2) = (C(L_1 = x, P_0/\sigma), C(L_2 = L_2^\xi(x), P_0/\sigma))$ on the boundary of the rate region $R_{ZF}(\mathbf{H}, P_0/\sigma, \xi)$.

For a given $(L_1 = x, L_2 = L_2^\xi(x))$ the corresponding information rate pair lies on the boundary of the proposed rate region $R_{ZF}(\mathbf{H}, P_0/\sigma, \xi)$. We denote this information rate pair by $(R_1^{Bd}(x, P_0/\sigma, \xi), R_2^{Bd}(x, P_0/\sigma, \xi))$. From (14), this information rate pair is given by

$$R_1^{Bd}(x, P_0/\sigma, \xi) \triangleq C(L = x, P_0/\sigma). \quad (16)$$

$$R_2^{Bd}(x, P_0/\sigma, \xi) \triangleq C(L = L_2^\xi(x), P_0/\sigma). \quad (17)$$

This then completely characterizes the boundary of the rate region $R_{ZF}(\mathbf{H}, P_0/\sigma, \xi)$, which is given by⁸

$$\begin{aligned} R_{ZF}^{Bd}(\mathbf{H}, P_0/\sigma, \xi) &\triangleq \cup_{0 \leq x \leq L_1^{\max}(\xi)} (R_1^{Bd}(x, P_0/\sigma, \xi), R_2^{Bd}(x, P_0/\sigma, \xi)) \\ &= \cup_{0 \leq x \leq L_1^{\max}(\xi)} (C(x, P_0/\sigma), C(L_2^\xi(x), P_0/\sigma)) \end{aligned} \quad (18)$$

It is noted that the analysis done in this paper is applicable to any placement of the users and the LEDs. Subsequently, we follow the following convention that, by *LED 1* we shall refer to the LED whose channel vector has a higher inclination angle (from the u_1 axis) than the inclination angle of the channel vector of the other LED.

Let the inclination of the vector \mathbf{h}_1 and \mathbf{h}_2 from the u_1 axis be θ_1 and θ_2 respectively (see Fig. 2). From our definition of LED 1 and LED 2 (see the above paragraph), it follows that $\theta_1 > \theta_2$. Therefore it follows that $\tan \theta_1 > \tan \theta_2$. Since

$$\tan \theta_1 = h_{21}/h_{11}, \quad \tan \theta_2 = h_{22}/h_{12}. \quad (19)$$

Hence, $\tan \theta_1 > \tan \theta_2$ implies that

$$\begin{aligned} h_{21}/h_{11} - h_{22}/h_{12} &> 0, \\ h_{11}h_{22} - h_{12}h_{21} &< 0, \quad \text{i.e.} \\ \det(\mathbf{H}) &< 0 \end{aligned} \quad (20)$$

In the following proposition, we first compute the maximum value of L_1 and subsequently we derive the maximum value of L_2 for each value of L_1 .

Proposition 1. *The largest possible value of L_1 (i.e., length of the interval \mathcal{U}_1) such that there exists a rectangle*

⁸From (16) and (17) it is clear that the exact computation of $R_1^{Bd}(x, P_0/\sigma, \xi)$ and $R_2^{Bd}(x, P_0/\sigma, \xi)$ requires the computation of $L_2^\xi(x)$ for which we derive closed form expressions in the next section. Computation of $R_1^{Bd}(x, P_0/\sigma, \xi)$ and $R_2^{Bd}(x, P_0/\sigma, \xi)$ also requires us to compute the $C(L, P_0/\sigma)$ function which is done numerically.

$Rect(L_1, L_2, D(\mathbf{H}, \xi))$ ($L_2 \geq 0$) which lies completely inside the parallelogram $R_{//}(\mathbf{H})$, is given by

$$\begin{aligned} L_1^{\max}(\xi) &\triangleq \max_{\substack{L_1 \geq 0, L_2 \geq 0 \\ Rect(L_1, L_2, D(\mathbf{H}, \xi)) \subset R_{//}(\mathbf{H})}} L_1 \\ &= \begin{cases} \frac{-2\xi \det(\mathbf{H})}{\max(h_{21}, h_{22})}, & 0 \leq \xi \leq 1/2 \\ \frac{-2(1-\xi) \det(\mathbf{H})}{\max(h_{21}, h_{22})}, & 1/2 \leq \xi \leq 1. \end{cases} \end{aligned} \quad (21)$$

Proof: See Appendix A. ■

It is clear from (21) in Proposition 1 that $L_1^{\max}(\xi)$ is a continuous function of ξ and $L_1^{\max}(\xi) = L_1^{\max}(1 - \xi)$.

Remark 1. *The function $L_1^{\max}(\xi)$ is a continuous function of ξ and is symmetric about $\xi = 1/2$, i.e.*

$$L_1^{\max}(\xi) = L_1^{\max}(1 - \xi), \quad 0 \leq \xi \leq 1 \quad (22)$$

From (21) it is clear that since $\det(\mathbf{H}) < 0$ (see (20)) $L_1^{\max}(x)$ is linearly increasing for $0 \leq \xi \leq 1/2$ and is linearly decreasing for $1/2 \leq \xi \leq 1$. Hence $L_1^{\max}(\xi)$ has a unique maximum at $\xi = 1/2$.

Remark 2. *The function $L_1^{\max}(\xi)$ has its unique maximum at $\xi = 1/2$, i.e.*

$$\arg \max_{0 \leq \xi \leq 1} L_1^{\max}(\xi) = 1/2 \quad (23)$$

Proposition 2. *For a given $L_1 = x \in [0, L_1^{\max}(\xi)]$, the largest possible $L_2 \geq 0$ such that there exists a rectangle $Rect(x, L_2, D(\mathbf{H}, \xi)) \subset R_{//}(\mathbf{H})$, is given by*

$$\begin{aligned} L_2^\xi(x) &\triangleq \max_{\substack{L_2 \geq 0 \\ Rect(x, L_2, D(\mathbf{H}, \xi)) \subset R_{//}(\mathbf{H})}} L_2 \\ &= 2 \min(L_2^{up, \xi}(x), L_2^{down, \xi}(x)), \end{aligned} \quad (24)$$

where $L_2^{up, \xi}(x)$ is given by

Case I: $0 \leq \xi \leq \frac{h_{11}}{h_{11} + h_{12}}$

$$L_2^{up, \xi}(x) = \begin{cases} \frac{-\xi \det(\mathbf{H}) - \frac{\xi}{2} h_{21}}{h_{11}}, & 0 \leq x \leq L_1^{\max}(\xi) \end{cases} \quad (25)$$

Case II: $\frac{h_{11}}{h_{11} + h_{12}} \leq \xi \leq 1$

$$L_2^{up, \xi}(x) = \begin{cases} \frac{-(1-\xi) \det(\mathbf{H}) - \frac{\xi}{2} h_{22}}{h_{12}}, & 0 \leq x \leq \eta_3(\xi) \\ \frac{-\xi \det(\mathbf{H}) - \frac{\xi}{2} h_{21}}{h_{11}}, & \eta_3(\xi) \leq x \leq L_1^{\max}(\xi) \end{cases} \quad (26)$$

where $\eta_3(\xi) \triangleq 2\xi h_{12} - 2(1 - \xi)h_{11}$.

$L_2^{down, \xi}(x)$ is given by

Case I: $0 \leq \xi \leq \frac{h_{12}}{h_{11} + h_{12}}$

$$L_2^{down, \xi}(x) = \begin{cases} \frac{-\xi \det(\mathbf{H}) - \frac{\xi}{2} h_{22}}{h_{12}}, & 0 \leq x \leq \eta_4(\xi) \\ \frac{-(1-\xi) \det(\mathbf{H}) - \frac{\xi}{2} h_{21}}{h_{11}}, & \eta_4(\xi) \leq x \leq L_1^{\max}(\xi) \end{cases} \quad (27)$$

where $\eta_4(\xi) \triangleq 2(1 - \xi)h_{12} - 2\xi h_{11}$.

Case II: $\frac{h_{12}}{h_{11}+h_{12}} \leq \xi \leq 1$

$$L_2^{\text{down},\xi}(x) = \begin{cases} \frac{-(1-\xi)\det(\mathbf{H}) - \frac{\sigma}{2}h_{21}}{h_{11}}, & 0 \leq x \leq L_1^{\max}(\xi) \end{cases} \quad (28)$$

Proof: See Appendix B. ■

Lemma 1. *The function $L_2^\xi(x)$ ($0 \leq x \leq L_1^{\max}(\xi)$) is a monotonically decreasing and continuous function of x .*

Proof: From Proposition 2 it is clear that for a given ξ both $L_2^{\text{up},\xi}(x)$ and $L_2^{\text{down},\xi}(x)$ are continuous and monotonically decreasing function of x . From this it follows that $L_2^\xi(x) = 2 \min(L_2^{\text{up},\xi}(x), L_2^{\text{down},\xi}(x))$ is a continuous and decreases monotonically with increasing x . ■

Lemma 2. *The proposed rate region boundary $R_{ZF}^{\text{Bd}}(\mathbf{H}, P_0/\sigma, \xi)$ is Pareto-optimal. That is, for any two rate pairs (a, b) and (a', b') on the boundary $R_{ZF}^{\text{Bd}}(\mathbf{H}, P_0/\sigma, \xi)$, if $a' \geq a$ then it must be true that $b' \leq b$ and if $b' \leq b$ then it must be true that $a' \geq a$.*

Proof: Let (a, b) and (a', b') be any two rate pairs on the boundary $R_{ZF}^{\text{Bd}}(\mathbf{H}, P_0/\sigma, \xi)$ such that $a' \geq a$. Then from ((16) and (17)) it follows that there exists $0 \leq x \leq L_1^{\max}(\xi)$ and $0 \leq x' \leq L_1^{\max}(\xi)$ such that $a = C(x, P_0/\sigma)$, $b = C(L_2^\xi(x), P_0/\sigma)$ and $a' = C(x', P_0/\sigma)$, $b' = C(L_2^\xi(x'), P_0/\sigma)$, where the functions $C(x, P_0/\sigma)$ is defined in (13). From Result (2), we know that for a given P_0/σ , $C(x, P_0/\sigma)$ is a continuous and monotonically increasing function of its first argument. Since $C(x', P_0/\sigma) = a' \geq a = C(x, P_0/\sigma)$, it follows that $x' \geq x$. From Lemma 1, we know that $L_2^\xi(x)$ is a monotonically decreasing function of x , and therefore $L_2^\xi(x') \leq L_2^\xi(x)$, and hence $b' = C(L_2^\xi(x'), P_0/\sigma) \leq C(L_2^\xi(x), P_0/\sigma) = b$. Similarly, it can also be shown that, if $b' \leq b$ then it must be true that $a' \geq a$. This completes the proof. ■

Lemma 3. *For a given $0 \leq \xi \leq 1$ and $x \in [0, L_1^{\max}(\xi)]$, the function $L_2^\xi(x)$ is symmetric about $\xi = 1/2$, i.e.*

$$L_2^\xi(x) = L_2^{1-\xi}(x), \quad 0 \leq \xi \leq 1, x \in [0, L_1^{\max}(\xi)]. \quad (29)$$

Proof: See Appendix C. ■

Using Lemma 3 along with the definition of the rate region boundary in (18) we get the following result.

Result 3. *The proposed rate region boundary $R_{ZF}^{\text{Bd}}(\mathbf{H}, P_0/\sigma, \xi)$ is symmetric about $\xi = 1/2$, i.e.*

$$R_{ZF}^{\text{Bd}}(\mathbf{H}, P_0/\sigma, \xi) = R_{ZF}^{\text{Bd}}(\mathbf{H}, P_0/\sigma, (1-\xi)), \quad \forall \xi \in [0, 1]. \quad (30)$$

The following theorem shows that for $0 \leq \xi \leq 1$, the largest rate region is achieved when $\xi = 1/2$.

Theorem 1. *For a fixed $\xi \in [0, 1]$,*

$$R_{ZF}(\mathbf{H}, P_0/\sigma, \xi) \subseteq R_{ZF}(\mathbf{H}, P_0/\sigma, 1/2). \quad (31)$$

Proof: See Appendix D. ■

The proposed rate region boundary $R_{ZF}^{\text{Bd}}(\mathbf{H}, P_0/\sigma, \xi)$ can be used to compute many practical operating points. Consider a case where we are interested in finding the largest achievable

rate pair (R_1, R_2) such that $R_2 = \alpha R_1$. This operating point could make sense, if for example the average data throughput requested by user 2 is α times that of the throughput requested by user 1.

Moreover, for a given $\alpha > 0$ and P_0/σ , the maximum achievable rate pair of the form $(r, \alpha r)$ is given by $(R_{\max}^\alpha(\xi), \alpha R_{\max}^\alpha(\xi))$ where $R_{\max}^\alpha(\xi)$ is defined as

$$R_{\max}^\alpha(\xi) \triangleq \max_{r | (r, \alpha r) \in R_{ZF}(\mathbf{H}, P_0/\sigma, \xi)} r. \quad (32)$$

Theorem 2. *$R_{\max}^\alpha(\xi)$ is unique and $(R_{\max}^\alpha(\xi), \alpha R_{\max}^\alpha(\xi))$ lies on the boundary $R_{ZF}^{\text{Bd}}(\mathbf{H}, P_0/\sigma, \xi)$.*

Proof: See Appendix E. ■

Remark 3. *From the proof in Appendix E it is clear that Theorem 2 is non-trivial as it depends on the monotonicity and continuity of $L_2^\xi(x)$, which is shown in Lemma 1. If Lemma 1 were not true, Theorem 2 would not hold.*

Result 4. *Using Theorem 2 and (30) of Result 3 it follows that for a given $\alpha > 0$, $R_{\max}^\alpha(\xi)$ is symmetric about $\xi = 1/2$, i.e.*

$$R_{\max}^\alpha(\xi) = R_{\max}^\alpha(1-\xi), \quad \forall \alpha > 0, \xi \in [0, 1]. \quad (33)$$

Corollary 2.1. *From the geometrical interpretation of Theorem 2 it follows that $(R_{\max}^\alpha(\xi), \alpha R_{\max}^\alpha(\xi))$ lies on the intersection of the straight line $R_2 = \alpha R_1$ and the rate region boundary $R_{ZF}^{\text{Bd}}(\mathbf{H}, P_0/\sigma, \xi)$. Further, from the Pareto-optimality of the proposed rate region boundary, it follows that there is only a unique point of intersection between the line $R_2 = \alpha R_1$ and $R_{ZF}^{\text{Bd}}(\mathbf{H}, P_0/\sigma, \xi)$.*

A. Maximum symmetric rate $R^{\text{sym}}(\xi)$

Note that for the special case of $\alpha = 1$, $R_{\max}^\alpha(\xi)$ is nothing but the maximum achievable symmetric rate which we shall denote by

$$R^{\text{sym}}(\xi) \triangleq R_{\max}^{\alpha=1}(\xi). \quad (34)$$

From Theorem 2 it is clear that the maximum symmetric rate is nothing but the largest rate R such that the rate pair (R, R) lies on the boundary $R_{ZF}^{\text{Bd}}(\mathbf{H}, P_0/\sigma, \xi)$. From the characterization of the boundary points in (18), it follows that there must exist $(x, L_2^\xi(x))$ for some $0 \leq x \leq L_1^{\max}(\xi)$ such that

$$R = C(x, P_0/\sigma), \quad \text{and} \quad R = C(L_2^\xi(x), P_0/\sigma) \quad (35)$$

and therefore

$$x = L_2^\xi(x) \quad (36)$$

since from Result 2 we know that $C(L, P_0/\sigma)$ is a continuous and monotonic function. From 14 it follows that there exists a rectangle $\text{Rect}(x, L_2^\xi(x), D(\mathbf{H}, \xi)) \subset R_{ZF}(\mathbf{H})$ corresponding to the rate pair (R, R) where x satisfies 36.

Since $x = L_2^\xi(x)$ it follows that this rectangle is in fact a square. Further, from the definition of $L_2^\xi(x)$ in (24) it follows that this is the largest sized square whose midpoint is at $D(\mathbf{H}, \xi)$ and has side length x .

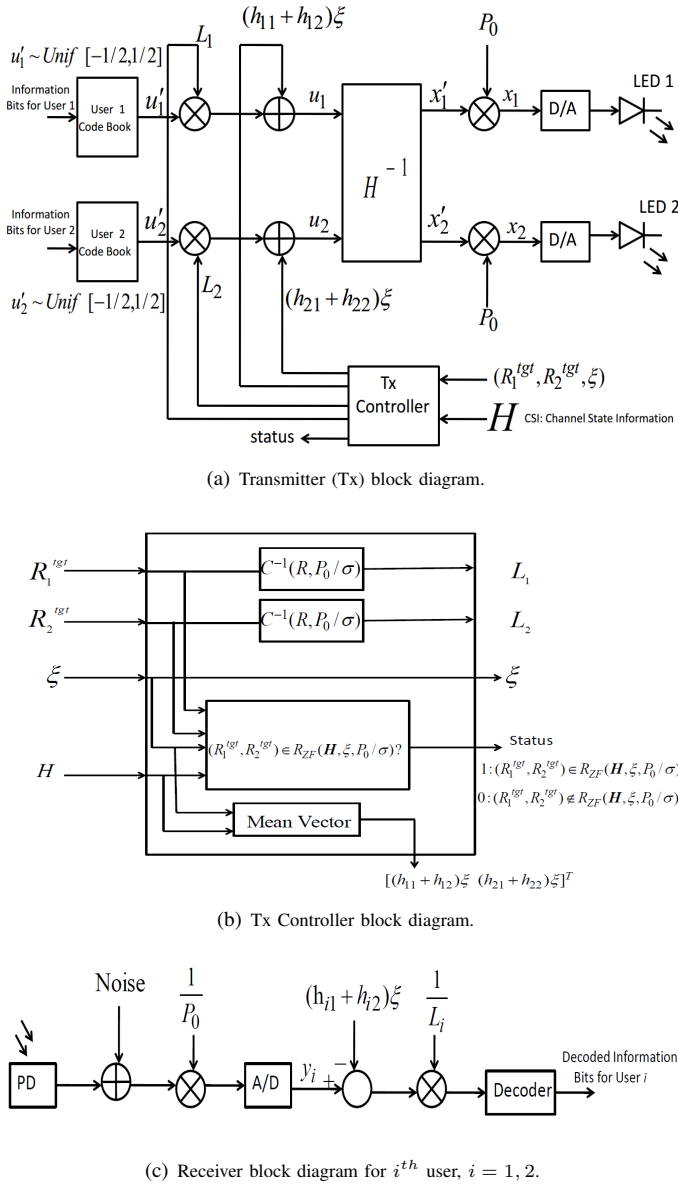


Fig. 3: A novel transceiver architecture for the proposed 2×2 MU-MISO VLC system with dimming Target of ξ and target rate pair (R_1^{tgt}, R_2^{tgt}) .

Hence, the maximum achievable symmetric rate corresponds to the largest sized square which is completely inside $R_{\text{ZF}}(\mathbf{H})$ and has its midpoint at $D(\mathbf{H}, \xi)$.

V. A NOVEL TRANSCIEVER ARCHITECTURE

In this section we propose a novel transceiver architecture for the practical implementation of the proposed 2×2 MU-MISO VLC system to achieve any rate pair $(R_1, R_2) \in R_{\text{ZF}}(\mathbf{H}, P_0/\sigma, \xi)$ (see Section IV), under a per-LED peak power constraint of P_0 and a controllable dimming target.

In Fig. 3, we have shown the block diagram of both the transmitter and the receiver. The block diagram in Fig. 3(a) depicts the transmitter, the block diagram in Fig. 3(b) depicts the controller for the transmitter which we call as Tx controller

and the block diagram in Fig. 3(c) depicts the receiver. The working of this transceiver is as follows.

Consider a scenario where the rate requested by User 1 and User 2 are R_1^{tgt} bpcu and R_2^{tgt} bpcu respectively and to satisfy the lighting requirement inside the room the required dimming target is ξ . We call this rate pair (R_1^{tgt}, R_2^{tgt}) , as the target rate pair of the system. The Tx controller first checks if this target rate pair lies in the proposed achievable rate region $R_{\text{ZF}}(\mathbf{H}, P_0/\sigma, \xi)$ (see Section IV). If the target rate pair lies inside the proposed achievable rate region, (i.e., $(R_1^{tgt}, R_2^{tgt}) \in R_{\text{ZF}}(\mathbf{H}, P_0/\sigma, \xi)$) then the Tx controller flags 1, otherwise it flags 0 (see status output of the Tx controller in Fig. 3(b)). If this flag is 1, then the Tx controller provides L_1 and L_2 , the lengths of the intervals \mathcal{U}_1 and \mathcal{U}_2 . From (15) we know that since $(R_1^{tgt}, R_2^{tgt}) \in R_{\text{ZF}}(\mathbf{H}, P_0/\sigma, \xi)$, there must exist some (L_1, L_2) such that $R_1^{tgt} = C(L_1, P_0/\sigma)$ and $R_2^{tgt} = C(L_2, P_0/\sigma)$. From Result 2 we also know that for a given P_0/σ , $C(x, P_0/\sigma)$ is a monotonic function of x , and therefore there exists a corresponding inverse function $C^{-1}(R, P_0/\sigma)$ such that $C^{-1}(C(L, P_0/\sigma), P_0/\sigma) = L$ and $C(C^{-1}(R, P_0/\sigma), P_0/\sigma) = R$. It then follows $L_i = C^{-1}(R_i^{tgt}, P_0/\sigma)$, $i = 1, 2$ see Fig. 3(c). In the Tx controller we also have a block which outputs the mean information symbol vector $\xi(\mathbf{h}_1 + \mathbf{h}_2) = [\xi(h_{11} + h_{12}) \quad \xi(h_{21} + h_{22})]^T$ (defined in (9)).

Further, in Fig. 3(a) the information bits for user 1 and user 2 are coded separately using independent codebooks each having i.i.d. codeword symbols which are uniformly distributed in $[-1/2, 1/2]$. The codeword symbols for user 1 and user 2 are denoted by u'_1 and u'_2 respectively (note that u_1 and u_2 are the information symbols for User 1 and User 2 respectively). From Section III, we know that the information symbols for the i^{th} user must be uniformly distributed in the interval \mathcal{U}_i i.e., $u_i \in \mathcal{U}_i = [\xi(h_{i1} + h_{i2}) - L_i/2, \xi(h_{i1} + h_{i2}) + L_i/2]$ (since the horizontal length of the rectangle corresponding to the rate pair (R_1^{tgt}, R_2^{tgt}) is L_1 , the vertical length of this rectangle is L_2 and its midpoint is $D(\mathbf{H}, \xi)$). Therefore, starting with the codeword symbol u'_i we can get the information symbol u_i by

$$u_i = L_i u'_i + \xi(h_{i1} + h_{i2}), \quad i = 1, 2. \quad (37)$$

This is also shown in Fig. 3. The information vector $[u_1 \ u_2]^T$ is then precoded with H^{-1} and scaled by P_0 to give the transmit signal vector $[x_1 \ x_2]^T$. It is noted that the proposed transmitter architecture in Fig. 3(a) allows us to use the same channel encoder/codebook irrespective of the dimming target ξ . This is because the effect of the dimming control is only in shifting the mean of the information symbols (u_1, u_2) (see the adds in Fig 3(a)).⁹

At the receiver after performing the operations shown in Fig. 3(c), we obtain the received vector as given by (5).

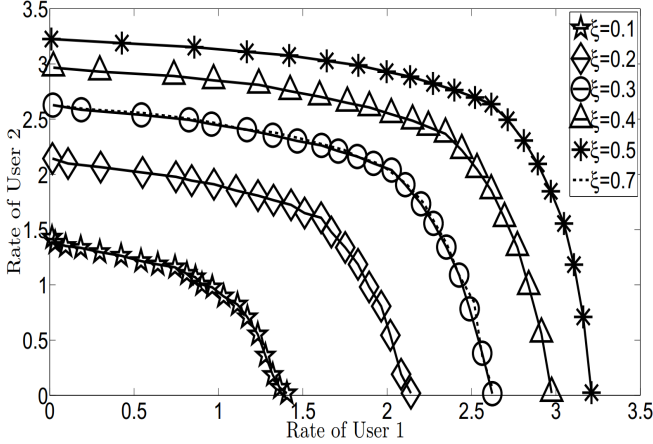
VI. NUMERICAL RESULTS AND DISCUSSIONS

In this section, we present numerical results in support of the results reported in previous sections. For all numerical results we consider an indoor office room environment where

⁹Note that different target rates can be achieved by the same codebook through puncturing of the codewords.

TABLE I: System Parameters used for Simulation

PD area	1 cm ²
Receiver Field of View (FOV)	60 [deg.]
Refractive index of a lens at the PD	1.5
Semi-angle at half power	70 [deg.]

Fig. 4: Rate region boundary, $R_{ZF}^{Bd}(\mathbf{H}, P_0/\sigma, \xi)$ for different values of dimming target, ξ .

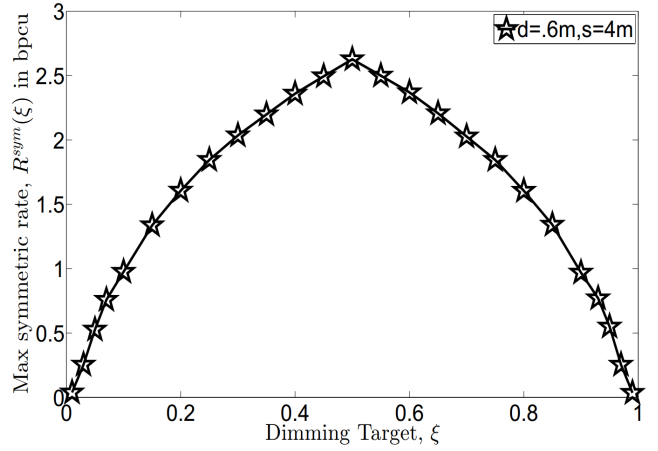
the room is 5 m \times 5 m and its height is 3 m. The two LEDs are attached to the ceiling and the two PDs (users) are placed at a height of 50 cm from the floor of the room. The two LEDs and the PDs lie in a plane perpendicular to the floor of the plane. The LEDs are placed 60 cm apart and the ratio $\frac{P_0}{\sigma}$ is fixed to 70 dB. The channel gains are modeled for an indoor line of sight (LOS) channel. The other parameters used for simulation are given in Table I. All these parameters and the channel model are taken from prior work [3], [14], [17], [18].

In Fig. 4, for a LED separation of 0.6 m and PD (user) separation of 4 m such that the placement of both the LEDs and the PDs is symmetric¹⁰, we plot the proposed rate region boundary $R_{ZF}^{Bd}(\mathbf{H}, P_0/\sigma, \xi)$ (see 18), for $\xi = 0.1, 0.2, 0.3, 0.4, 0.5, 0.7$.

For a given ξ , it is observed that the boundary is indeed Pareto-optimal as is stated in Lemma 2. We also observe that as ξ increases from $\xi = 0.1$ to $\xi = 0.5$, the rate region expands and then it shrinks with further increase in ξ from $\xi = 0.5$ onwards to $\xi = 1$. We have also observed that rate region boundary is same for both $\xi = 0.3$ and $\xi = 1 - 0.3 = 0.7$ as is stated in Result 3 (see the dotted line and the solid line marked with circle in Fig. 4). It is also observed that $\xi = 1/2$ gives us the largest rate region as is stated in Theorem 1. The expansion/shrinking of the rate region with changing ξ is explained in the following.

For a given ξ , the points on the rate region boundary correspond to rectangles in the $u_1 - u_2$ plane having their midpoints at $D(\mathbf{H}, \xi)$, i.e., on the diagonal $(\mathbf{h}_1 + \mathbf{h}_2)$ and at a distance of $\xi\|\mathbf{h}_1 + \mathbf{h}_2\|$ from the origin. As ξ increases, the midpoint of the rectangles move away from the origin

¹⁰Both the line segment joining the two users and the line segment joining the two LEDs have the same perpendicular bisector.

Fig. 5: Plot between Maximum Symmetric Rate and dimming Target, ξ .

and towards the interior of the parallelogram $R_{//}(\mathbf{H})$. This allows us to fit bigger rectangles and hence the rate region expands. As ξ is increased beyond $\xi = 0.5$ the midpoint of the rectangles moves towards the other end of the diagonal $(\mathbf{h}_1 + \mathbf{h}_2)$ and hence the size of the rectangles reduces thereby shrinking the rate region.

In Fig. 5, for a fixed user separation of $s = 4$ m, an LED separation of $d = 60$ cm and symmetric placement of LEDs and PDs, we plot the maximum achievable symmetric rate $R^{sym}(\xi) \triangleq R_{max}^{\alpha=1}(\xi)$ as a function of varying $\xi \in [0, 1]$. We numerically find this operating point by considering all possible points in the $R_1 - R_2$ plane which lie in the achievable rate region and also lie on the line $R_2 = R_1$. Then among all these possible points we choose the one which has the largest component along the R_1 axis. From the figure it is observed that the variation in the maximum symmetric rate with change in the dimming target ξ is small when ξ is around $1/2$, as compared to when $\min(\xi, 1 - \xi)$ is small. For example, when ξ is reduced from $\xi = 1/2$ to $\xi = 0.4$ (i.e., 20% reduction), the corresponding maximum symmetric rate drops only by 11%. However when ξ is reduced by 20% from $\xi = 0.07$ to $\xi = 0.056$, the maximum symmetric rate decreases by approximately 25%. From this it appears that the maximum symmetric rate is lesser sensitive to variations in the dimming target around $\xi = 1/2$ as compared to variations around smaller values of ξ . It is also observed that symmetric rate $R^{sym}(\xi)$ is symmetric about $\xi = 1/2$ as is stated in Result 4 (symmetric rate is nothing but $R_{max}^{\alpha}(\xi)$ for $\alpha = 1$).

We next study the variation in the maximum symmetric rate when the two users (PDs) are moved along a line parallel to the ceiling (at a height of 50 cm above the floor) while the two LEDs are stationary and fixed to the ceiling with a fixed separation of 60 cm between them and the dimming target is also fixed to $\xi = 0.1$. Further, the two LEDs and the two PDs are co-planar. In Fig. 6, we plot the symmetric rate on the vertical axis as a function of the displacement¹¹ of the two users from the origin (origin is the point of intersection of the

¹¹Displacement is nothing but the distance of the user from the origin (see Fig. 1).

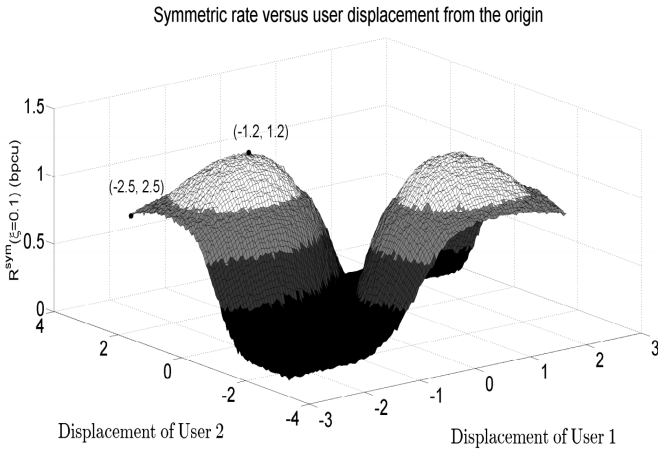


Fig. 6: Maximum symmetric rate vs displacement of the two users from the origin.

Percentage loss in $R^{sym}(\xi)$ vs users displacement from their optimum location $(-1.2, 1.2)/(1.2, -1.2)$

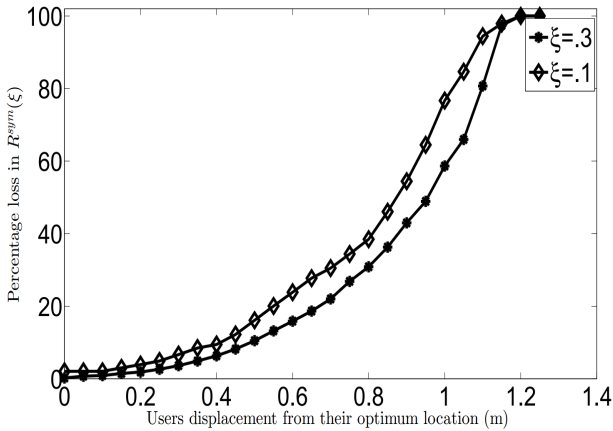


Fig. 7: Plot between percentage loss in $R^{sym}(\xi)$ and users displacement from their optimum location.

perpendicular bisector of the line joining the LEDs with the line joining the two users, see Fig. 1). In Fig. 6 a positive displacement implies that the user PD is located on the right side of the origin and vice versa (see Fig. 1).

It is observed that the maximum symmetric rate is almost zero if the displacement of both the users is same, i.e., the two users are almost co-located. In the figure this is represented by the dark black region. This is expected since in that case the channels to the users is also the same and hence the performance of the ZF precoder degrades. From the figure we observe that starting with both the users at the origin, as user 2 moves towards the right and User 1 moves towards left the maximum symmetric rate increases sharply (in the figure the colour changes from dark black to light black to gray as the displacement vector moves from $(0, 0)$ to $(-1.2, 1.2)$). This happens because as the users move away from each other, their channels become distinct i.e., the angles between the vectors \mathbf{h}_1 and \mathbf{h}_2 increases and hence the area of $R_{//}(\mathbf{H})$ increases. This results in an increase in the largest sized square that can be fit into $R_{//}(\mathbf{H})$ with center at $D(\mathbf{H}, \xi)$. This then implies that the maximum symmetric rate would also increase

(see the discussion in Section IV-A for the correspondence between the largest square and the maximum symmetric rate). With further increase in the separation between the two users the angular separation between the channel vectors does not increase as sharply as before. At the same time, due to increased path loss from the LEDs to the users, the area of $R_{//}(\mathbf{H})$ starts decreasing which results in the decrease in the maximum symmetric rate. This can be seen in the figure, as the colour changes back from white to gray, as we move from the displacement vector $(-1.2, 1.2)$ to $(-2.5, 2.5)$. This shows that the maximum symmetric rate is dependent on the location of the users and therefore there is an *optimal location*¹² for both the users which results in the highest symmetric rate. In Fig. 6 the optimum location is $(-1.2, 1.2)$, or $(1.2, -1.2)$.

Next in Fig. 7, for a fixed LED separation of 60 cm we plot the percentage loss in the maximum symmetric rate $R^{sym}(\xi)$ (w.r.t. the symmetric rate at the optimum location) with the users' displacement from their optimum location for two different values of $\xi = 0.1, 0.3$.

It is observed that the percentage loss increases with increasing displacement of the PDs from their optimal location. Further, the increase in the percentage loss is small when the displacement is small as compared to when the displacement is large. For example, with $\xi = 0.3$, the percentage loss increases only by 6% as the displacement increases from 0 cm to 40 cm. However with a further increase in displacement from 40 cm to 80 cm, the percentage loss increases sharply from 6% to 30%. A similar behavior is also observed with $\xi = 0.1$, though for a given displacement the loss is greater when $\xi = 0.1$ as compared to when $\xi = 0.3$. A practical application of this study could be in defining *coverage zones* for the PDs, i.e., the maximum allowable displacement for a fixed desired upper limit on the percentage loss. For example, in the current setup with $\xi = 0.3$, for a 20% upper limit on the percentage loss, the maximum allowable displacement is roughly 70 cm. It therefore appears that indoor VLC systems allow for a lot of flexibility in the movement of the user terminals without significant loss in the information rate.

VII. CONCLUSION

We have proposed an achievable rate region for the 2×2 MU-MISO broadcast VLC channel under per-LED peak power constraint and dimming control. The boundary of the proposed rate region has been analytically characterized. We propose a novel transceiver architecture to implement such systems. Interestingly, the design of encoder/codebook is independent of the dimming target, which reduces the complexity of the transceiver. Work done in this paper reveals that, in an indoor setting, the two users have enough mobility around their optimal placement without sacrificing their information rates. Our work can also be applied to a 2-D setting, where the users are allowed to move in a plane rather than being restricted to a line.

¹²By the optimum user location we mean the displacement vector of the users at which we get maximum $R^{sym}(\xi)$.

APPENDIX A
PROOF OF PROPOSITION 1

Proof: Under the condition in (20), to find $L_1^{\max}(\xi)$ we need to consider three scenarios that cover all geometrically possible parallelograms $R_{//}(\mathbf{H})$: (a) ($h_{11} < h_{12}$ and $h_{21} > h_{22}$); (b) ($h_{21} \leq h_{22}$); and (c) ($h_{12} \leq h_{11}$ and $h_{21} > h_{22}$).

For a given dimming target, ξ , let L_3 denote the length of the longest line segment parallel to the u_1 -axis lying completely inside $R_{//}(\mathbf{H})$ and whose midpoint coincides with the point $D(\mathbf{H}, \xi)$ ($D(\mathbf{H}, \xi)$ is defined in (10)). For any rectangle $Rect(L_1, L_2, D(\mathbf{H}, \xi)) \subset R_{//}(\mathbf{H})$, its side along the u_1 axis is a line segment inside $R_{//}(\mathbf{H})$. From the definition of L_3 , it follows that $L_1 \leq L_3$ for any rectangle $Rect(L_1, L_2, D(\mathbf{H}, \xi)) \subset R_{//}(\mathbf{H})$. Additionally, the longest line segment of length L_3 corresponds to a rectangle $Rect(L_3, L_2 = 0, D(\mathbf{H}, \xi)) \subset R_{//}(\mathbf{H})$. Hence, it is clear that $L_1^{\max}(\xi) = L_3$, i.e.

$$\begin{aligned} L_1^{\max}(\xi) &\triangleq \max_{\substack{L_1 \geq 0, L_2 \geq 0 \\ Rect(L_1, L_2, D(\mathbf{H}, \xi)) \subset R_{//}(\mathbf{H})}} L_1 \\ &= \max_{\{L_1 > 0 | Rect(L_1, L_2 = 0, D(\mathbf{H}, \xi)) \subset R_{//}(\mathbf{H})\}} L_1 \quad (38) \end{aligned}$$

In the following, we firstly evaluate the expression for $L_1^{\max}(\xi)$ for scenario (a), i.e., when the channel gains satisfy ($h_{11} < h_{12}$ and $h_{21} > h_{22}$). Towards this end, we partition $R_{//}(\mathbf{H})$ into three regions, Region $i, i = 1, 2, 3$, as is shown in Fig. 8. We now derive an expression for $L_1^{\max}(\xi)$ depending upon the region where $D(\mathbf{H}, \xi)$ lies. In Fig. 8 we denote $D(\mathbf{H}, \xi)$ by the point P if $D(\mathbf{H}, \xi)$ lies in Region 1, by the point Q if $D(\mathbf{H}, \xi)$ lies in Region 2 and by the point S if $D(\mathbf{H}, \xi)$ lies in Region 3. Next, we compute $L_1^{\max}(\xi)$ when $D(\mathbf{H}, \xi)$ lies in Region 1.

Computation of $L_1^{\max}(\xi)$ when $P = D(\mathbf{H}, \xi) \in$ Region 1 :

The point $D(\mathbf{H}, \xi)$ belongs to Region 1 if and only if

$$0 \leq OP \leq OT, \quad (39)$$

where the point T denote point of intersection of the diagonal OB and CC' . Further, the line CC' is the line parallel to the u_1 -axis. Next, by looking at the right angle triangle OT_1T in Fig. 8, it follows that $OT = TT_1/\sin \gamma$, where γ denotes inclination of the diagonal, OB , of the parallelogram $R_{//}(\mathbf{H})$ from the u_1 -axis. Since, from Fig. 8, $TT_1 = h_{22}$, and $\sin \gamma = (h_{21} + h_{22})/OB$, it follows that

$$OT = \frac{h_{22} OB}{h_{21} + h_{22}} \quad (40)$$

Since the point P is nothing but the point $D(\mathbf{H}, \xi)$, from (10), it follows that $OP = \xi OB$. Using $OP = \xi OB$ and (40) in (39) we have that $D(\mathbf{H}, \xi) \in$ Region 1 if and only if

$$0 \leq \xi \leq \frac{h_{22}}{h_{21} + h_{22}}, \quad (41)$$

For all such values of the dimming target, ξ , satisfying (41), it follows that $D(\mathbf{H}, \xi) \in$ Region 1. Next, we evaluate $L_1^{\max}(\xi)$ when $0 \leq \xi \leq h_{22}/(h_{21} + h_{22})$.

Since $L_1^{\max}(\xi)$ is the length of the line segment parallel to the u_1 -axis having its midpoint at point P and lying

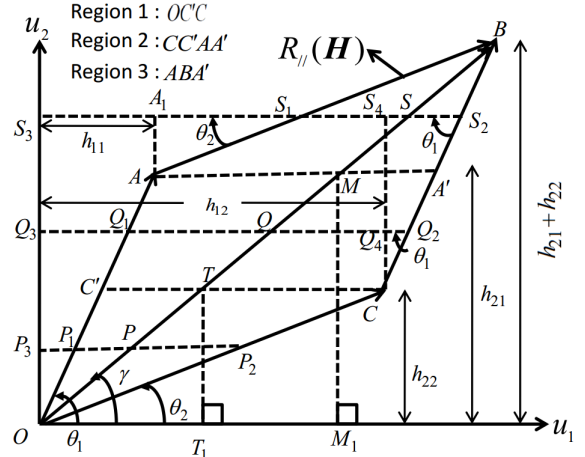


Fig. 8: Partition of the parallelogram $OABC \triangleq R_{//}(\mathbf{H})$ into three different regions for the scenario ($h_{11} < h_{12}$ and $h_{21} > h_{22}$). Note that AA' and CC' are both parallel to the u_1 axis.

completely inside $R_{//}(\mathbf{H})$, it follows that

$$L_1^{\max}(\xi) = 2 \min(PP_1, PP_2), \quad (42)$$

where both the line segments PP_1 and PP_2 are parallel to the u_1 -axis. Further, P_1 lies on the line OA whereas P_2 lies on the line OC as shown in Fig. 8. Next, we evaluate PP_1 and PP_2 . To this end, from Fig. 8, we compute the length of the line segment PP_1 as follows

$$\begin{aligned} PP_1 &= PP_3 - P_1P_3 \\ &\stackrel{(a)}{=} \xi(h_{11} + h_{12}) - OP_3/\tan \theta_1 \\ &\stackrel{(b)}{=} \xi(h_{11} + h_{12}) - \xi(h_{21} + h_{22})h_{11}/h_{21} \\ &= \xi(h_{12}h_{21} - h_{11}h_{22})/h_{21} = -\xi \det(\mathbf{H})/h_{21}, \quad (43) \end{aligned}$$

where step (a) follows from the fact that, PP_3 is equal to the co-ordinate of the point $D(\mathbf{H}, \xi)$ along the u_1 -axis and therefore from (10), we have $PP_3 = \xi(h_{11} + h_{12})$. In step (a) we have also used the fact that since OP_1P_3 is a right angle triangle having $\angle OP_3P_1 = \theta_1$. Hence, it follows that $P_1P_3 = OP_3/\tan \theta_1$. Step (b) also follows from two facts. Firstly, OP_3 is equal to the co-ordinate of the point $D(\mathbf{H}, \xi)$ along the u_2 -axis and therefore from (10), we have that $OP_3 = \xi(h_{21} + h_{22})$ and secondly, from (19), we know that $\tan \theta_1 = h_{21}/h_{11}$. Similarly from Fig. 8, we calculate the length of PP_2 as follows

$$\begin{aligned} PP_2 &= P_2P_3 - PP_3 \\ &\stackrel{(a)}{=} OP_3/\tan \theta_2 - \xi(h_{11} + h_{12}) \\ &\stackrel{(b)}{=} \xi(h_{21} + h_{22})h_{12}/h_{22} - \xi(h_{11} + h_{12}) \\ &= \xi(h_{12}h_{21} - h_{11}h_{22})/h_{22} = -\xi \det(\mathbf{H})/h_{22}, \quad (44) \end{aligned}$$

where step (a) follows from the fact that, PP_3 is equal to the co-ordinate of the point $D(\mathbf{H}, \xi)$ along the u_1 -axis and therefore from (10), we have that $PP_3 = \xi(h_{11} + h_{12})$. In step (a) we have also used the fact that OP_3P_2 is a right angle triangle having $\angle OP_2P_3 = \theta_2$. Hence, it follows that $P_2P_3 = OP_3/\tan \theta_2$. Step (b) follows from two facts.

Firstly, OP_3 is equal to the co-ordinate of the point $D(\mathbf{H}, \xi)$ along the u_2 -axis and therefore from (10), we have that $OP_3 = \xi(h_{21} + h_{22})$ and secondly, $\tan \theta_2 = h_{22}/h_{12}$. Using (43) and (44) in (42) we see that when $0 \leq \xi \leq h_{22}/(h_{21} + h_{22}) = \min(h_{21}, h_{22})/(h_{21} + h_{22})$ (since $h_{21} > h_{22}$ in scenario (a)), we have

$$L_1^{\max}(\xi) = -2 \xi \det(\mathbf{H}) \min\left(\frac{1}{h_{21}}, \frac{1}{h_{22}}\right) = \frac{-2 \xi \det(\mathbf{H})}{\max(h_{22}, h_{21})}. \quad (45)$$

Computation of $L_1^{\max}(\xi)$ when $Q = D(\mathbf{H}, \xi) \in \text{Region 2}$:

Point $Q = D(\mathbf{H}, \xi)$ lies in Region 2= $CC'AA'$ if and only if

$$OT \leq OQ \leq OM, \quad (46)$$

where M is the point of intersection of the line segment AA' and the diagonal OB (see Fig. 8). In the following we firstly show that $D(\mathbf{H}, \xi) \in \text{Region 2}$ if and only if

$$\frac{h_{22}}{h_{21} + h_{22}} \leq \xi \leq \frac{h_{21}}{h_{21} + h_{22}}. \quad (47)$$

Towards this end, we firstly derive an expression for OM . From the right angle triangle OM_1M in Fig. 8, we know that $OM = MM_1/\sin \gamma$ and since $MM_1 = h_{21}$, $\sin \gamma = (h_{21} + h_{22})/OB$. We have

$$OM = \frac{h_{21} OB}{h_{21} + h_{22}}. \quad (48)$$

Since the point Q is nothing but the point $D(\mathbf{H}, \xi)$, from (10), we have $OQ = \xi OB$ and from (40), it follows that $OT = \frac{h_{22} OB}{h_{21} + h_{22}}$. In (46), we substitute OQ by ξOB , OM by the R.H.S in (48) and OT by $\frac{h_{22} OB}{h_{21} + h_{22}}$ to get

$$\begin{aligned} \frac{h_{22} OB}{(h_{21} + h_{22})} \leq \xi OB \leq \frac{h_{21} OB}{(h_{21} + h_{22})} \\ \frac{h_{22}}{(h_{21} + h_{22})} \leq \xi \leq \frac{h_{21}}{(h_{21} + h_{22})} \end{aligned} \quad (49)$$

For all such values of the dimming target, ξ , satisfying (49), it follows that $D(\mathbf{H}, \xi) \in \text{Region 2}$. Next, we evaluate $L_1^{\max}(\xi)$ when $h_{22}/(h_{21} + h_{22}) \leq \xi \leq h_{21}/(h_{21} + h_{22})$. For this scenario, from Fig. 8 we see that

$$L_1^{\max}(\xi) = 2 \min(QQ_1, QQ_2), \quad (50)$$

where construction of QQ_1 and QQ_2 is similar to the construction of PP_1 and PP_2 (see Fig. 8), except the fact that Q_2 lies on CB instead of OC . Next, we evaluate QQ_1 and QQ_2 . To this end, using the similar steps as for the evaluation of PP_1 (see (43)) we have,

$$QQ_1 = QQ_3 - Q_1Q_3 = \frac{-\xi \det(\mathbf{H})}{h_{21}}. \quad (51)$$

However, evaluation of QQ_2 is not the same as evaluation of PP_2 , as the point Q_2 lies on the line segment CB whereas the point P_2 lies on the line OC . Towards this end, using Fig. 8,

we evaluate QQ_2 as follows

$$\begin{aligned} QQ_2 &= Q_3Q_2 - Q_3Q \\ &= Q_3Q_4 + Q_4Q_2 - Q_3Q \\ &= h_{12} + \frac{CQ_4}{\tan \theta_1} - \xi(h_{11} + h_{12}) \\ &= h_{12} + \frac{\xi(h_{21} + h_{22}) - h_{22}}{(h_{21}/h_{11})} - \xi(h_{11} + h_{12}) \\ &= \frac{-\det(\mathbf{H})(1 - \xi)}{h_{21}} \end{aligned} \quad (52)$$

Using (51) and (52) in (50), we see that when $h_{22}/(h_{21} + h_{22}) \leq \xi \leq h_{21}/(h_{21} + h_{22})$, i.e. $\min(h_{21}, h_{22})/(h_{21} + h_{22}) \leq \xi \leq \max(h_{21}, h_{22})/(h_{21} + h_{22})$ (since $h_{21} > h_{22}$ in scenario (a)), we have

$$L_1^{\max}(\xi) = \frac{-2 \det(\mathbf{H}) \min(\xi, (1 - \xi))}{h_{21}} \quad (53)$$

$$\stackrel{(a)}{=} -2 \det(\mathbf{H}) \frac{\min(\xi, (1 - \xi))}{\max(h_{21}, h_{22})}, \quad (54)$$

where step (a) follows from the fact that $h_{21} = \max(h_{21}, h_{22})$, since for scenario (a), we know that $h_{21} > h_{22}$.

Computation of $L_1^{\max}(\xi)$ when $S = D(\mathbf{H}, \xi) \in \text{Region 3}$:

Point $S = D(\mathbf{H}, \xi)$ lies in Region 3= $AA'B$ if and only if $OM \leq OS \leq OB$. Using (48) $\left(\frac{OM}{OB} = \frac{h_{21}}{h_{21} + h_{22}}\right)$ and the fact that $OS = \xi OB$ (from (10)), we have

$$h_{21}/(h_{21} + h_{22}) \leq \xi \leq 1. \quad (55)$$

Next, we evaluate $L_1^{\max}(\xi)$ when $h_{21}/(h_{21} + h_{22}) \leq \xi \leq 1$. From Fig. 8 it is clear that when $S = D(\mathbf{H}, \xi) \in \text{Region 3}$ then $L_1^{\max}(\xi)$ is given by

$$L_1^{\max}(\xi) = 2 \min(SS_1, SS_2), \quad (56)$$

where S_1 and S_2 are the intersections of the straight line parallel to the u_1 axis passing through S , with the line segment AB and CB respectively. Next, we evaluate SS_1 and SS_2 . To this end, using similar steps as for the evaluation of QQ_2 (see (52)) we have,

$$\begin{aligned} SS_2 &= S_3S_2 - S_3S \\ &= S_3S_4 + S_4S_2 - S_3S \\ &= \frac{-\det(\mathbf{H})(1 - \xi)}{h_{21}} \end{aligned} \quad (57)$$

However, evaluation of SS_1 is not same as evaluation of QQ_1 , as the point S_1 lies on the line segment AB whereas the point Q_1 lies on the line OA . Towards the evaluation of SS_1 , using Fig. 8, we have

$$\begin{aligned} SS_1 &= SS_3 - S_1S_3 \\ &= \xi(h_{11} + h_{12}) - (S_3A_1 + A_1S_1) \\ &= \xi(h_{11} + h_{12}) - \left(h_{11} + \frac{AA_1}{\tan \theta_2}\right) \\ &= \xi(h_{11} + h_{12}) - \left(h_{11} + \frac{\xi(h_{21} + h_{22}) - h_{21}}{(h_{22}/h_{12})}\right) \\ &= \frac{-\det(\mathbf{H})(1 - \xi)}{h_{22}} \end{aligned} \quad (58)$$

Using (57) and (58) in (56), we see that when

$h_{21}/(h_{21} + h_{22}) \leq \xi \leq 1$, i.e. $\max(h_{21}, h_{22})/(h_{21} + h_{22}) \leq \xi \leq 1$ (since $h_{21} > h_{22}$ in scenario (a)), we have

$$L_1^{\max}(\xi) = -2 \det(\mathbf{H})(1 - \xi) \min\left(\frac{1}{h_{21}}, \frac{1}{h_{22}}\right) \quad (59)$$

$$\underline{(a)} \quad \frac{-2 \det(\mathbf{H})(1 - \xi)}{\max(h_{21}, h_{22})},$$

where step (a) follows from the fact that $h_{21} = \max(h_{21}, h_{22})$, since for scenario (a), we know that $h_{21} > h_{22}$.

Therefore for the scenario (a), we have the expression of $L_1^{\max}(\xi)$ as follows

$$L_1^{\max}(\xi) = \begin{cases} \frac{-2\xi \det(\mathbf{H})}{\max(h_{21}, h_{22})}, & 0 \leq \xi \leq \eta_1 \triangleq \frac{\min(h_{21}, h_{22})}{(h_{21} + h_{22})} \\ \frac{-2 \det(\mathbf{H}) \min(\xi, (1 - \xi))}{\max(h_{21}, h_{22})}, & \eta_1 \leq \xi \leq \eta_2 \triangleq \frac{\max(h_{21}, h_{22})}{(h_{21} + h_{22})} \\ \frac{-2(1 - \xi) \det(\mathbf{H})}{\max(h_{21}, h_{22})}, & \eta_2 \leq \xi \leq 1. \end{cases} \quad (60)$$

Since

$$\eta_1 \triangleq \frac{\min(h_{21}, h_{22})}{(h_{21} + h_{22})} \leq 1/2 \quad (61)$$

and

$$\eta_2 \triangleq \frac{\max(h_{21}, h_{22})}{(h_{21} + h_{22})} \geq 1/2, \quad (62)$$

where the above two inequalities follows from the simple mathematical manipulations, and therefore the expression in (60) can be further simplified. To this end, we consider two cases based on the values of ξ .

Case (a): $0 \leq \xi \leq 1/2$

For this case we know that $\xi \leq (1 - \xi)$ and hence

$$\min(\xi, (1 - \xi)) = \xi \quad (63)$$

Since from (61) and (62), we know that $\eta_1 \leq 1/2$ and $\eta_2 \geq 1/2$ and hence, for $0 \leq \xi \leq 1/2$ from (60) and (63) we have

$$L_1^{\max}(\xi) = \frac{-2\xi \det(\mathbf{H})}{\max(h_{21}, h_{22})} \quad (64)$$

Case (b): $1/2 \leq \xi \leq 1$

For this case we know that $\xi \geq (1 - \xi)$ and hence

$$\min(\xi, (1 - \xi)) = (1 - \xi) \quad (65)$$

Since from (61) and (62), we know that $\eta_1 \leq 1/2$ and $\eta_2 \geq 1/2$ and hence, for $1/2 \leq \xi \leq 1$ from (60) and (65) we have

$$L_1^{\max}(\xi) = \frac{-2(1 - \xi) \det(\mathbf{H})}{\max(h_{21}, h_{22})}. \quad (66)$$

Therefore from (64) and (66) the final expression of $L_1^{\max}(\xi)$ for scenario (a) is as follows

$$L_1^{\max}(\xi) = \begin{cases} \frac{-2\xi \det(\mathbf{H})}{\max(h_{21}, h_{22})}, & 0 \leq \xi \leq 1/2 \\ \frac{-2(1 - \xi) \det(\mathbf{H})}{\max(h_{21}, h_{22})}, & 1/2 \leq \xi \leq 1 \end{cases} \quad (67)$$

Using similar arguments as for scenario (a), we evaluate $L_1^{\max}(\xi)$ for **Scenario (b):** ($h_{21} \leq h_{22}$); and for **Scenario (c):** ($h_{12} \leq h_{11}$ and $h_{21} > h_{22}$) as follows.

To this end, we first partition $R_{//}(\mathbf{H})$ into three regions as shown in Fig. 9. Next, we denote $D(\mathbf{H}, \xi)$ by the point P if

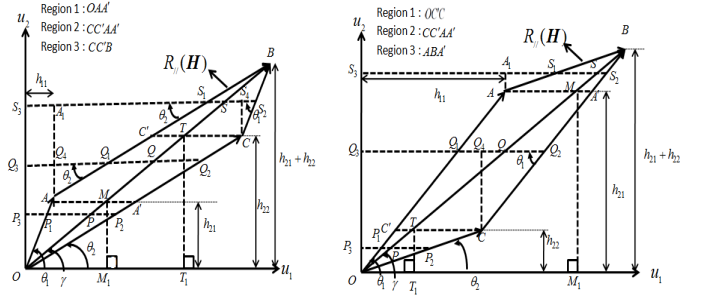


Fig. 9: Partition of the parallelogram $OABC \triangleq R_{//}(\mathbf{H})$ into three different regions for the scenario (b) ($h_{21} \leq h_{22}$); and scenario (c) ($h_{12} \leq h_{11}$ and $h_{21} > h_{22}$) (left to right).

$D(\mathbf{H}, \xi)$ lies in Region 1, by the point Q if $D(\mathbf{H}, \xi)$ lies in Region 2 and by the point S if $D(\mathbf{H}, \xi)$ lies in Region 3.

Using (48) and (40) we can also show that the point $D(\mathbf{H}, \xi)$ lies in Region 1 if and only if $0 \leq \xi \leq \frac{\min(h_{21}, h_{22})}{h_{21} + h_{22}}$, $D(\mathbf{H}, \xi)$ lies in Region 2 iff $\frac{\min(h_{21}, h_{22})}{h_{21} + h_{22}} \leq \xi \leq \frac{\max(h_{21}, h_{22})}{h_{21} + h_{22}}$ and it lies in Region 3 iff $\frac{\max(h_{21}, h_{22})}{h_{21} + h_{22}} \leq \xi \leq 1$. Next, we evaluate $L_1^{\max}(\xi)$ when $D(\mathbf{H}, \xi)$ lies in Region i , $i = 1, 2, 3$.

Following similar steps as for scenario (a), from Fig. 9 it follows that when $D(\mathbf{H}, \xi) \in$ Region 1, i.e., when $0 \leq \xi \leq \frac{\min(h_{21}, h_{22})}{(h_{21} + h_{22})}$

$$L_1^{\max}(\xi) = \frac{-2\xi \det(\mathbf{H})}{\max(h_{21}, h_{22})} \quad (68)$$

Similarly, using Fig. 9 it can be shown that when $D(\mathbf{H}, \xi) \in$ Region 2, i.e., when $\frac{\min(h_{21}, h_{22})}{(h_{21} + h_{22})} \leq \xi \leq \frac{\max(h_{21}, h_{22})}{(h_{21} + h_{22})}$

$$L_1^{\max}(\xi) = -2 \det(\mathbf{H}) \frac{\min(\xi, (1 - \xi))}{\max(h_{21}, h_{22})}. \quad (69)$$

Further, using Fig. 9 it can be shown that when $D(\mathbf{H}, \xi) \in$ Region 3, i.e., when $\frac{\max(h_{21}, h_{22})}{(h_{21} + h_{22})} \leq \xi \leq 1$

$$L_1^{\max}(\xi) = \frac{-2(1 - \xi) \det(\mathbf{H})}{\max(h_{21}, h_{22})}. \quad (70)$$

Following the steps used to arrive at (67) from (60) in scenario(a), for scenario (b) and (c) also we get the same final expression for $L_1^{\max}(\xi)$ as in (67). This completes the proof. ■

APPENDIX B PROOF OF PROPOSITION 2

Proof:

Similar to proposition 1, for proving proposition 2, we consider three mutually exclusive scenarios. (a) ($h_{11} < h_{12}$ and $h_{21} > h_{22}$); (b) ($h_{21} \leq h_{22}$); and (c) ($h_{12} \leq h_{11}$ and $h_{21} > h_{22}$). Moreover, from the definition of LED 1 and LED 2, it follows that, the channel matrix satisfies (20), i.e. $\det(\mathbf{H}) < 0$. For a fixed $(\mathbf{H}, P_0/\sigma, \xi)$, in the following, for a given $L_1 = x$, $0 \leq x \leq L_1^{\max}(\xi)$, we derive the expression for the maximum L_2 , (i.e., length of the side of the rectangle along the u_2 -axis (vertical length)), such that there exists a

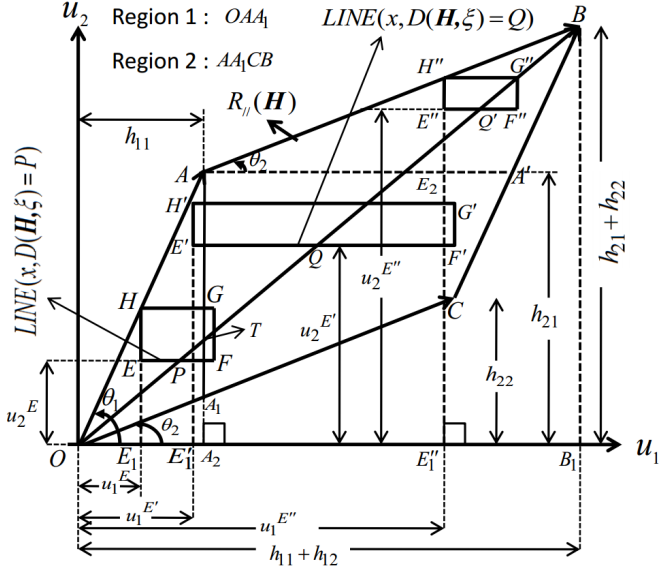


Fig. 10: Evaluation of $L_2^{up,\xi}(x)$ for Scenario (a) ($h_{11} < h_{12}$ and $h_{21} > h_{22}$).

rectangle $Rect(L_1 = x, L_2, D(\mathbf{H}, \xi)) \subset R_{//}(\mathbf{H})$, i.e.

$$L_2^\xi(x) \triangleq \max_{L_2 \geq 0} L_2. \quad (71)$$

$$Rect(x, L_2, D(\mathbf{H}, \xi)) \subset R_{//}(\mathbf{H})$$

To this end, for a fixed ξ ,¹³ and given $L_1 = x$, we construct all such possible rectangles $Rect(L_1 = x, L_2, D(\mathbf{H}, \xi)) \subset R_{//}(\mathbf{H})$ and among them we choose the rectangle having the maximum possible vertical length.

To get this rectangle we first construct a horizontal line segment of the length x parallel to the u_1 -axis such that its midpoint coincides with the point $D(\mathbf{H}, \xi)$. We denote this line segment by $LINE(x, D(\mathbf{H}, \xi))$, i.e.

$$LINE(x, D(\mathbf{H}, \xi)) \triangleq \{v = (v_1, v_2) \in \mathbb{R}^2 \mid v_1 \in S_1, v_2 \in S_2\}, \quad (72)$$

where $S_1 \triangleq \{v_1 \in \mathbb{R} \mid |v_1 - \xi(h_{11} + h_{12})| \leq (x/2)\}$ and $S_2 \triangleq \{v_2 \in \mathbb{R} \mid v_2 = \xi(h_{21} + h_{22})\}$. Since $x \leq L_1^{\max}(\xi)$, from the definition of $L_1^{\max}(\xi)$ it follows that $LINE(x, D(\mathbf{H}, \xi))$ lies completely inside $R_{//}(\mathbf{H})$.

Given any horizontal line segment of length x parallel to the u_1 -axis, any rectangle inside $R_{//}(\mathbf{H})$ having this line segment as one of its side can be constructed in two possible ways, either by extending it vertically downwards or extending it vertically upwards.¹⁴ Subsequently, we shall refer to these construction methods as “downward extension” and “upward extension”.

Using this for a given $L_2 > 0$ we can construct a rectangle by extending the line segment $LINE(x, D(\mathbf{H}, \xi))$ vertically

upwards. We denote this rectangle by

$$Rect^{up}(x, L_2, D(\mathbf{H}, \xi)) \triangleq Rect(x, L_2, D(\mathbf{H}, \xi) + C_0), \quad (73)$$

where $C_0 \triangleq (0, L_2/2)$. Let $L_2^{up,\xi}(x)$ denote the largest possible vertical length of all such rectangles which lie completely inside $R_{//}(\mathbf{H})$ and are constructed by the upward extension of the line segment $LINE(x, D(\mathbf{H}, \xi))$, i.e.

$$L_2^{up,\xi}(x) \triangleq \max_{L_2 \geq 0} L_2. \quad (74)$$

$$Rect^{up}(L_1 = x, L_2, D(\mathbf{H}, \xi)) \subset R_{//}(\mathbf{H})$$

Similarly, we construct any rectangle of vertical length $L_2 \geq 0$ by extending the line segment $LINE(x, D(\mathbf{H}, \xi))$ vertically downwards. We denote this rectangle by

$$Rect^{down}(x, L_2, D(\mathbf{H}, \xi)) \triangleq Rect(x, L_2, D(\mathbf{H}, \xi) + C_1), \quad (75)$$

where $C_1 \triangleq (0, -L_2/2)$. Let $L_2^{down,\xi}(x)$ denote the largest possible vertical length of all such rectangles which lie completely inside $R_{//}(\mathbf{H})$ and are constructed using the “downward extension” method, i.e.

$$L_2^{down,\xi}(x) \triangleq \max_{L_2 \geq 0} L_2. \quad (76)$$

$$Rect^{down}(x, L_2, D(\mathbf{H}, \xi)) \subset R_{//}(\mathbf{H})$$

$L_2^\xi(x)$ is the maximum possible vertical length of any rectangle lying completely inside $R_{//}(\mathbf{H})$ with horizontal side length equal to x and having its mid point at $D(\mathbf{H}, \xi)$, which is the midpoint of the line segment $LINE(x, D(\mathbf{H}, \xi))$. Equivalently, such a maximal rectangle¹⁵ must be symmetric about the line segment $LINE(x, D(\mathbf{H}, \xi))$. Since such a maximal rectangle $Rect(x, L_2^\xi(x), D(\mathbf{H}, \xi))$ lies inside $R_{//}(\mathbf{H})$, from (74) and (76) it follows that

$$Rect(x, L_2^\xi(x), D(\mathbf{H}, \xi)) \subset S_3 \cup S_4,$$

where $S_3 \triangleq Rect^{up}(x, L_2^{up,\xi}(x), D(\mathbf{H}, \xi))$ and $S_4 \triangleq Rect^{down}(x, L_2^{down,\xi}(x), D(\mathbf{H}, \xi))$ and $S_3 \cap S_4 = LINE(x, D(\mathbf{H}, \xi))$. Further since the maximal rectangle $Rect(x, L_2^\xi(x), D(\mathbf{H}, \xi))$ has the maximum possible vertical length and is symmetric about $LINE(x, D(\mathbf{H}, \xi))$, it follows that $L_2^\xi(x)/2 = L_2^{up,\xi}(x)$ if $L_2^{up,\xi}(x) \leq L_2^{down,\xi}(x)$, and $L_2^\xi(x)/2 = L_2^{down,\xi}(x)$ if $L_2^{down,\xi}(x) \leq L_2^{up,\xi}(x)$, i.e.

$$L_2^\xi(x) = 2 \min(L_2^{down,\xi}(x), L_2^{up,\xi}(x)). \quad (77)$$

We next derive expressions for $L_2^{up,\xi}(x)$ and $L_2^{down,\xi}(x)$ for $0 \leq x \leq L_1^{\max}(\xi)$ for a fixed $0 \leq \xi \leq 1$. We firstly consider scenario (a) ($h_{11} < h_{12}$ and $h_{21} > h_{22}$).

A. Computation of $L_2^{up,\xi}(x)$ for scenario (a)

Towards this end, we divide $R_{//}(\mathbf{H})$ into two regions, Region $i, i = 1, 2$, namely Region 1 = OAA_1 and Region 2 = AA_1CB (see Fig. 10). Note that in Fig. 10, the straight line AA_1A_2 is parallel to the u_2 -axis and A_1 is the point of intersection of this line segment with the side OC of $R_{//}(\mathbf{H})$. Next, we evaluate expressions for $L_2^{up,\xi}(x)$ depending upon

¹³Once we fix ξ , location of the point $D(\mathbf{H}, \xi)$ gets fixed (see (10)).

¹⁴By extending a horizontal line segment vertically downwards/upwards, we mean that we create a rectangle by drawing two vertical lines from the end points of this horizontal line segment in the downward/upward direction and then connecting the other two end points of these two vertical lines to form a rectangle.

¹⁵By the maximal rectangle we mean, the rectangle with the maximum possible vertical length for a given horizontal length and which lies completely inside the rectangle $R_{//}(\mathbf{H})$.

the region where $D(\mathbf{H}, \xi)$ lies. In Fig. 10, we denote $D(\mathbf{H}, \xi)$ by the point P if $D(\mathbf{H}, \xi)$ lies in Region 1 and by the point Q/Q' if $D(\mathbf{H}, \xi)$ lies in Region 2.

Computation of $L_2^{up,\xi}(x)$ when $D(\mathbf{H}, \xi) = P \in \text{Region 1}$:
The point $D(\mathbf{H}, \xi) = P \in \text{Region 1} = OAA_1$ iff

$$0 \leq OP \leq OT, \quad (78)$$

where T is the point of intersection of the line segment AA_2 with the diagonal OB (see Fig. 10). Next, we evaluate expression for OT . Towards this end, from the similarity of the triangles OTA_2 and OBB_1 it follows that $\frac{OT}{OB} = \frac{OA_2}{OB_1}$. Further, from Fig. 10, it follows that $OA_2 = h_{11}$ and $OB_1 = h_{11} + h_{12}$ and therefore we have,

$$OT = \frac{h_{11}}{h_{11} + h_{12}} OB. \quad (79)$$

Since the point P is nothing but the point $D(\mathbf{H}, \xi)$, from (10) we have $OP = \xi OB$. Therefore, using (79) and $OP = \xi OB$ in (78) we have, $D(\mathbf{H}, \xi) \in \text{Region 1}$ iff $0 \leq \xi \leq \frac{h_{11}}{h_{11} + h_{12}}$.

When $0 \leq \xi \leq \frac{h_{11}}{h_{11} + h_{12}}$, from (74) it follows that for evaluating $L_2^{up,\xi}(x)$, we need to construct rectangles $Rect^{up}(x, L_2, D(\mathbf{H}, \xi))$ using the ‘‘upward extension’’ of the line segment $LINE(x, D(\mathbf{H}, \xi) = P) = EF$ as shown in Fig. 10. $L_2^{up,\xi}(x)$ is then the largest possible vertical length of all such rectangles which lie inside $R_{//}(\mathbf{H})$. From Fig. 10, it is clear that during the upward extension of the line EF , with increasing vertical length L_2 of the constructed rectangle $Rect^{up}(x, L_2, D(\mathbf{H}, \xi))$, the vertically upward line from E will be the first to move out of $R_{//}(\mathbf{H})$ when compared to the vertical line from F . Hence it follows that in Fig. 10, for $x = EF$ and $0 \leq \xi \leq \frac{h_{11}}{h_{11} + h_{12}}$, we have $L_2^{up,\xi}(x) = EH$. To evaluate EH , we firstly denote the (u_1, u_2) coordinates of the point E by (u_1^E, u_2^E) . From the definition of $LINE(x, D(\mathbf{H}, \xi))$ and (10) it is clear that

$$u_1^E = \xi(h_{11} + h_{12}) - x/2, \quad u_2^E = \xi(h_{21} + h_{22}). \quad (80)$$

When $0 \leq \xi \leq \frac{h_{11}}{h_{11} + h_{12}}$ and $0 \leq x \leq L_1^{\max}(\xi)$, using Fig. 10, EH is computed as follows

$$\begin{aligned} L_2^{up,\xi}(x) &= EH = E_1H - E_1E \\ &= u_1^E \tan \theta_1 - u_2^E \\ &\stackrel{(a)}{=} \left(\xi(h_{11} + h_{12}) - \frac{x}{2} \right) \frac{h_{21}}{h_{11}} - \xi(h_{21} + h_{22}) \\ &= \frac{-\xi \det(\mathbf{H}) - \frac{x}{2} h_{21}}{h_{11}} \end{aligned} \quad (81)$$

where E_1 is the point of intersection of the extension of the line segment EH and the u_1 -axis (see Fig. 10). Step (a) follows from (80) and (19).

Computation of $L_2^{up,\xi}(x)$ when $D(\mathbf{H}, \xi) = Q \in \text{Region 2}$:

Point $D(\mathbf{H}, \xi) = Q$ lies in Region 2 = AA_1CB if and only if $OT \leq OQ \leq OB$. Since Q denote the point $D(\mathbf{H}, \xi)$, from (10) we have, $OQ = \xi OB$ and from (79) we have $OT = \frac{h_{11}OB}{h_{11} + h_{12}}$. Hence, it follows that $D(\mathbf{H}, \xi)$ lies in Region 2 iff $\frac{h_{11}}{h_{11} + h_{12}} \leq \xi \leq 1$. We next evaluate $L_2^{up,\xi}(x)$ when ξ lies in this interval.

From (74), it follows that for evaluating $L_2^{up,\xi}(x)$, we need

to construct rectangles $Rect^{up}(x, L_2, Q = D(\mathbf{H}, \xi))$ using the ‘‘upward extension’’ of the line segment $LINE(x, Q = D(\mathbf{H}, \xi))$ as shown in Fig. 10. $L_2^{up,\xi}(x)$ is then the largest possible vertical length of all such rectangles which lie inside $R_{//}(\mathbf{H})$. From Fig. 10, it is clear that during the upward extension of the line segment $LINE(x, Q = D(\mathbf{H}, \xi))$, the upper left vertex of the constructed rectangle having the largest vertical length will either intersect with the side OA of $R_{//}(\mathbf{H})$ or with the side AB of $R_{//}(\mathbf{H})$ (see rectangles $E'F'G'H'$ and $E''F''G''H''$ in Fig. 10). The upper left vertex intersects with the side OA if and only if the lower left vertex of the constructed rectangle, (i.e., the leftmost point of the line segment $LINE(x, D(\mathbf{H}, \xi))$) (see E' in Fig. 10) lies inside Region 1, i.e.

$$\begin{aligned} u_1^{D(\mathbf{H}, \xi)} - x/2 &\leq h_{11}, \text{ i.e.} \\ 2\xi h_{12} - 2(1 - \xi)h_{11} &\leq x, \end{aligned} \quad (82)$$

where u_1 coordinate of the point $D(\mathbf{H}, \xi)$ is denoted by $u_1^{D(\mathbf{H}, \xi)}$. From (10), we know that $u_1^{D(\mathbf{H}, \xi)} = \xi(h_{11} + h_{12})$. On the other hand, the upper left vertex intersects with the side AB of $R_{//}(\mathbf{H})$ if and only if the lower left vertex of the constructed rectangle, i.e., the leftmost point of the line segment $LINE(x, Q' = D(\mathbf{H}, \xi))$ (see E'' in Fig. 10) lies inside Region 2, i.e.

$$\begin{aligned} u_1^{D(\mathbf{H}, \xi)} - x/2 &\geq h_{11}, \text{ i.e.} \\ x &\leq 2\xi h_{12} - 2(1 - \xi)h_{11}. \end{aligned} \quad (83)$$

From the above, we know that when x satisfies (82), i.e. $2\xi h_{12} - 2(1 - \xi)h_{11} \leq x$, the lower left vertex of the constructed rectangle lies in Region 1 and the upper left vertex lies on the side OA . Hence, we have

$$\begin{aligned} L_2^{up,\xi}(x) &= E'H' = E_1'H' - E_1'E' \\ &= \frac{-\xi \det(\mathbf{H}) - \frac{x}{2} h_{21}}{h_{11}} \end{aligned} \quad (84)$$

Similarly, when x satisfies (83), i.e. $2\xi h_{12} - 2(1 - \xi)h_{11} \geq x$, the lower left vertex of the constructed rectangle lies in Region 2 and the upper left vertex lies on the side AB . Hence, we have

$$\begin{aligned} L_2^{up,\xi}(x) &= E''H'' \\ &= E_1''H'' - E_1''E'' \\ &= E_1''E_2 + E_2H'' - E_1''E'' \\ &\stackrel{(a)}{=} h_{21} + AE_2 \tan \theta_2 - E_1''E'' \\ &\stackrel{(b)}{=} h_{21} + (u_1^{E''} - h_{11}) \tan \theta_2 - u_2^{E''} \\ &\stackrel{(c)}{=} h_{21} + \left(\xi(h_{11} + h_{12}) - \frac{x}{2} - h_{11} \right) \frac{h_{22}}{h_{12}} - \xi(h_{21} + h_{22}) \\ &= \frac{-(1 - \xi) \det(\mathbf{H}) - \frac{x}{2} h_{22}}{h_{12}}, \end{aligned}$$

where E_2 is the point of intersection of the line $E''H''$ with AA' and $(u_1^{E''}, u_2^{E''})$ are the (u_1, u_2) coordinates of the point E'' . Step (a) follows from right angle triangle AE_2H'' . Step (b) follows from the fact that, $AE_2 = u_1^{E''} - h_{11}$ and $E_1E'' = u_2^{E''}$. In step (c) the expression for $u_1^{E''}$ and $u_2^{E''}$ follows from the definition of $LINE(x, D(\mathbf{H}, \xi))$ in (72) and (10) and the value of $\tan \theta_2$ follows from (19). Therefore, when $D(\mathbf{H}, \xi) \in$

$E'F'J'K'$ and $E''F''J''K''$ in Fig. 11). The lower right vertex intersects with the side CB if and only if the upper right vertex of the constructed rectangle, (i.e., the rightmost point of the line segment $LINE(x, D(\mathbf{H}, \xi))$) (see F' in Fig. 11) lies inside Region 1, i.e.

$$\begin{aligned} u_1^{D(\mathbf{H}, \xi)} + x/2 &\geq h_{12}, \text{ i.e.} \\ x &\geq 2(1 - \xi)h_{12} - 2\xi h_{11}, \end{aligned} \quad (92)$$

where $u_1^{D(\mathbf{H}, \xi)}$ denote the u_1 coordinate of the point $D(\mathbf{H}, \xi)$. From (10) we know that $u_1^{D(\mathbf{H}, \xi)} = \xi(h_{11} + h_{12})$. On the other hand, the lower right vertex of the constructed rectangle intersects with the side OC of $R_{//}(\mathbf{H})$ if and only if the upper right vertex of the constructed rectangle (i.e., the rightmost point of the line segment $LINE(x, D(\mathbf{H}, \xi))$) (see F'' in Fig. 11) lies inside Region 2, i.e.

$$\begin{aligned} u_1^{D(\mathbf{H}, \xi)} + x/2 &\leq h_{12}, \text{ i.e.} \\ x &\leq 2(1 - \xi)h_{12} - 2\xi h_{11}. \end{aligned} \quad (93)$$

From the above, we know that when $x \leq 2(1 - \xi)h_{12} - 2\xi h_{11}$, the upper right vertex of the constructed rectangle lies in Region 2 and the lower right vertex lies on the side OC . Hence, we have $L_2^{down, \xi}(x) = F''J''$. Towards this end, we firstly denote the (u_1, u_2) coordinates of the point F'' by $(u_1^{F''}, u_2^{F''})$. From the definition of $LINE(x, D(\mathbf{H}, \xi))$ in (72) and from (10) we have

$$u_1^{F''} = \xi(h_{11} + h_{12}) + \frac{x}{2}, \quad u_2^{F''} = \xi(h_{21} + h_{22}). \quad (94)$$

Next, for $0 \leq \xi \leq h_{12}/(h_{11} + h_{12})$ and $0 \leq x \leq 2(1 - \xi)h_{12} - 2\xi h_{11}$, we evaluate expression for $L_2^{down, \xi}(x) = F''J''$ as follows.

$$\begin{aligned} L_2^{down, \xi}(x) &= F''J'' \\ &= F_1''F'' - F_1''J'' \\ &\stackrel{(a)}{=} u_2^{F''} - u_1^{F''} \tan \theta_2 \\ &\stackrel{(b)}{=} \xi(h_{21} + h_{22}) - \left(\xi(h_{11} + h_{12}) + \frac{x}{2} \right) \frac{h_{22}}{h_{12}} \\ &= \frac{-\xi \det(\mathbf{H}) - \frac{\pi}{2} h_{22}}{h_{12}}, \end{aligned} \quad (95)$$

where F_1'' is the point of intersection of the line $F''J''$ extended downward with the u_1 -axis (see Fig. 11). Step (a) follows from the two facts. Firstly, from the fact that $F_1''F''$ is the u_2 coordinate F'' , and secondly from the right angle triangle $OF_1''J''$, we have $\tan \theta_2 = \frac{F_1''J''}{u_1^{F''}}$, i.e. $F_1''J'' = u_1^{F''} \tan \theta_2$. Step (b) follows from (94) and (19).

On the other hand, when $x \geq 2(1 - \xi)h_{12} - 2\xi h_{11}$, the upper right vertex of the constructed rectangle lies in Region 1 and the lower right vertex lies on the side CB . Hence, we have $L_2^{down, \xi}(x) = F'J'$. Towards this end, we firstly denote the (u_1, u_2) coordinates of the point F' by $(u_1^{F'}, u_2^{F'})$. From the definition of $LINE(x, D(\mathbf{H}, \xi))$ in (72) and from (10) we have

$$u_1^{F'} = \xi(h_{11} + h_{12}) + \frac{x}{2}, \quad u_2^{F'} = \xi(h_{21} + h_{22}). \quad (96)$$

The steps involved in the evaluation of $F'J'$ is exactly the same as for the evaluation of FJ in (90). Hence, from Fig. 11

we have

$$\begin{aligned} L_2^{down, \xi}(x) &= F'J' \\ &= F_1'F' - F_1'J' \\ &= \frac{-(1 - \xi)\det(\mathbf{H}) - \frac{\pi}{2} h_{21}}{h_{11}}, \end{aligned} \quad (97)$$

Therefore, in scenario (a) ($h_{11} < h_{12}$ and $h_{21} > h_{22}$), from (90), (95) and (97) we finally have

$$L_2^{down, \xi}(x) = \begin{cases} \frac{-(1 - \xi)\det(\mathbf{H}) - \frac{\pi}{2} h_{21}}{h_{11}}, & \mu_2 \leq \xi \leq 1 \text{ and } 0 \leq x \leq L_1^{\max}(\xi) \\ \frac{-\xi \det(\mathbf{H}) - \frac{\pi}{2} h_{22}}{h_{12}}, & 0 \leq \xi \leq \mu_2 \text{ and } 0 \leq x \leq \eta_4(\xi) \\ \frac{-(1 - \xi)\det(\mathbf{H}) - \frac{\pi}{2} h_{21}}{h_{11}}, & 0 \leq \xi \leq \mu_2 \text{ and } \eta_4(\xi) \leq x \leq L_1^{\max}(\xi) \end{cases} \quad (98)$$

where $\mu_2 \triangleq \frac{h_{12}}{h_{11} + h_{12}}$ and $\eta_4(\xi) \triangleq 2(1 - \xi)h_{12} - 2\xi h_{11}$. In the following, we derive expressions for $L_2^{up, \xi}(x)$ and $L_2^{down, \xi}(x)$ for scenario (b) ($h_{21} \leq h_{22}$); and (c) ($h_{12} \leq h_{11}$ and $h_{21} > h_{22}$).

Similarly, for scenarios (b) and (c) also, by using the *upward* and *downward extension* methods we derive the expressions for $L_2^{up, \xi}(x)$ and $L_2^{down, \xi}(x)$ respectively by constructing rectangles which lie inside $R_{//}(\mathbf{H})$ and have the maximum possible vertical lengths for a given horizontal length. It turns out that the expression for $(L_2^{up, \xi}(x), L_2^{down, \xi}(x))$ is exactly the same as that for scenario (a). ■

APPENDIX C PROOF OF LEMMA 3

Proof: To prove (29) we consider its R.H.S. $L_2^{1 - \xi}(x)$. From (24) the R.H.S. is given by

$$L_2^{(1 - \xi)}(x) = 2 \min(L_2^{up, (1 - \xi)}(x), L_2^{down, (1 - \xi)}(x)), \quad (99)$$

where the expression for $L_2^{up, (1 - \xi)}(x)$ is given by,

Case I: For $0 \leq (1 - \xi) \leq \frac{h_{11}}{h_{11} + h_{12}}$, i.e. $\frac{h_{12}}{h_{11} + h_{12}} \leq \xi \leq 1$ From (25) we have

$$\begin{aligned} L_2^{up, (1 - \xi)}(x) &= \begin{cases} \frac{-(1 - \xi)\det(\mathbf{H}) - \frac{\pi}{2} h_{21}}{h_{11}}, & 0 \leq x \leq L_1^{\max}(1 - \xi) \\ \frac{-\xi \det(\mathbf{H}) - \frac{\pi}{2} h_{21}}{h_{11}}, & 0 \leq x \leq L_1^{\max}(\xi) \end{cases} \\ &\stackrel{(a)}{=} L_2^{down, \xi}(x), \end{aligned} \quad (100)$$

where step (a) follows from (22) and step (b) follows from (28).

Case II: For $\frac{h_{11}}{h_{11} + h_{12}} \leq (1 - \xi) \leq 1$, i.e. $0 \leq \xi \leq \frac{h_{12}}{h_{11} + h_{12}}$, from (26) we have

$$\begin{aligned} L_2^{up, (1 - \xi)}(x) &= \begin{cases} \frac{-\xi \det(\mathbf{H}) - \frac{\pi}{2} h_{22}}{h_{12}}, & 0 \leq x \leq \eta_3(1 - \xi) \\ \frac{-(1 - \xi)\det(\mathbf{H}) - \frac{\pi}{2} h_{21}}{h_{11}}, & \eta_3(1 - \xi) \leq x \leq L_1^{\max}(1 - \xi) \end{cases} \\ &\stackrel{(a)}{=} \begin{cases} \frac{-\xi \det(\mathbf{H}) - \frac{\pi}{2} h_{22}}{h_{12}}, & 0 \leq x \leq \eta_4(\xi) \\ \frac{-(1 - \xi)\det(\mathbf{H}) - \frac{\pi}{2} h_{21}}{h_{11}}, & \eta_4(\xi) \leq x \leq L_1^{\max}(\xi) \end{cases} \\ &\stackrel{(b)}{=} L_2^{down, \xi}(x), \end{aligned} \quad (101)$$

where step (a) follows from two facts, firstly that $\eta_3(1 - \xi) \triangleq 2(1 - \xi)h_{12} - 2\xi h_{11} = \eta_4(\xi)$ and secondly from (22). Step

(b) follows from (27). Therefore we have,

$$L_2^{up,(1-\xi)}(x) = L_2^{down,\xi}(x), \quad \xi \in [0, 1], x \in [0, L_1^{\max}(\xi)] \quad (102)$$

From (102) we also have

$$L_2^{up,\xi}(x) = L_2^{down,(1-\xi)}(x), \quad \xi \in [0, 1], x \in [0, L_1^{\max}(\xi)] \quad (103)$$

Using (102) and (103) in (99) we finally have

$$\begin{aligned} L_2^{(1-\xi)}(x) &= 2 \min(L_2^{up,(1-\xi)}(x), L_2^{down,(1-\xi)}(x)) \\ &= 2 \min(L_2^{down,\xi}(x), L_2^{up,\xi}(x)) \\ &\stackrel{(a)}{=} L_2^\xi(x) \\ &= L.H.S., \end{aligned} \quad (104)$$

where step (a) follows from (24). This therefore completes the proof. \blacksquare

APPENDIX D PROOF OF THEOREM 1

To Prove this theorem we need the following Lemma.

Lemma 4. For a fixed $x \in [0, L_1^{\max}(1/2)]$, the function $L_2^\xi(x)$ attains its maximum at $\xi = 1/2$, i.e.

$$L_2^\xi(x) \leq L_2^{1/2}(x) \quad \forall \quad \xi \in [f(x), 1/2] \quad (105)$$

where for any $0 \leq x \leq L_1^{\max}(1/2)$, $f(x)$ is the unique¹⁶ value such that

$$L_1^{\max}(f(x)) = x \quad \text{and} \quad f(x) \leq 1/2. \quad (106)$$

Proof: To prove Lemma 4 we consider two cases (a) $h_{12} \leq h_{11}$; and (b) $h_{12} \geq h_{11}$. From Lemma 3, we know that for a fixed $x \in [0, L_1^{\max}(1/2)]$, $L_2^\xi(x)$ is symmetric about $\xi = 1/2$, hence we consider ξ only in the range $[0, 1/2]$. The proof of Lemma 4 is as follows

Case(a) $h_{12} \leq h_{11}$:

$$h_{12} \leq h_{11}, \quad \text{i.e.} \quad 1/2 \leq \frac{h_{11}}{h_{11} + h_{12}}. \quad (107)$$

Since $\frac{h_{11}}{h_{11} + h_{12}} \geq 1/2$ and $\xi \in [0, 1/2]$, we have $\xi \leq \frac{h_{11}}{h_{11} + h_{12}}$. Therefore from (25) we have

$$L_2^{up,\xi}(x) = \frac{-\xi \det(\mathbf{H}) - \frac{\pi}{2} h_{21}}{h_{11}}, \quad 0 \leq x \leq L_1^{\max}(1/2). \quad (108)$$

From the above equation it is clear that $L_2^{up,\xi}(x)$ is an increasing function of $\xi \in [0, 1/2]$ and therefore for any $\xi \in [0, 1/2]$ we have

$$\xi \leq 1/2 \implies L_2^{up,\xi}(x) \leq L_2^{up,1/2}(x). \quad (109)$$

From (103) we know that $L_2^{up,\xi}(x) = L_2^{down,(1-\xi)}(x)$, and therefore for $\xi = 1/2$

$$L_2^{up,1/2}(x) = L_2^{down,1/2}(x). \quad (110)$$

¹⁶Uniqueness follows from the fact that $L_1^{\max}(\xi)$ is continuous, increases linearly when $\xi \in [0, 1/2]$, has a unique maximum at $\xi = 1/2$, and $L_1^{\max}(\xi) = L_1^{\max}(1 - \xi)$.

using (110) in (24) we have

$$L_2^{up,1/2}(x) = L_2^{down,1/2}(x) = L_2^{\xi=1/2}(x)/2 \quad (111)$$

and hence using this along with (109), for any fixed $x \in [0, L_1^{\max}(1/2)]$ we have

$$\begin{aligned} L_2^{up,\xi}(x) &\leq L_2^{\xi=1/2}(x)/2, \quad \text{i.e.} \\ 2 \min(L_2^{up,\xi}(x), L_2^{down,\xi}(x)) &\leq L_2^{\xi=1/2}(x), \quad \text{i.e.} \\ L_2^\xi(x) &\leq L_2^{\xi=1/2}(x). \end{aligned} \quad (112)$$

Therefore for case(a) ($h_{12} \leq h_{11}$) and $\xi \in [0, 1/2]$ finally we have

$$L_2^\xi(x) \leq L_2^{\xi=1/2}(x), \quad 0 \leq x \leq L_1^{\max}(1/2). \quad (113)$$

Case(b) $h_{11} \leq h_{12}$:

$$h_{11} \leq h_{12}, \quad \text{i.e.} \quad 1/2 \leq \frac{h_{12}}{h_{11} + h_{12}}. \quad (114)$$

For this case, in order to prove $L_2^\xi(x) \leq L_2^{\xi=1/2}(x)$, we further consider two different cases on the basis of the values of $x \in [0, L_1^{\max}(1/2)]$ (b.I): $x \in [0, h_{12} - h_{11}]$; and (b.II): $x \in [h_{12} - h_{11}, L_1^{\max}(1/2)]$.

case (b.I): $x \in [0, h_{12} - h_{11}]$

From (27) we have

$$\begin{aligned} \eta_4(\xi) &= 2(1 - \xi)h_{12} - 2\xi h_{11} \\ &= 2h_{12} - 2\xi(h_{11} + h_{12}). \end{aligned} \quad (115)$$

From the above equation it is clear that $\eta_4(\xi)$ is monotonically decreasing with $0 \leq \xi \leq 1/2$ and therefore we have

$$\begin{aligned} \eta_4(1/2) &\leq \eta_4(\xi) \leq \eta_4(0) \\ h_{12} - h_{11} &\leq \eta_4(\xi) \leq 2h_{12} \end{aligned} \quad (116)$$

and since we know that $x \in [0, h_{12} - h_{11}]$, hence for any value of $\xi \in [0, 1/2]$, x will always be less than $\eta_4(\xi)$, i.e. $x \leq \eta_4(\xi)$. Therefore from (27) we have

$$L_2^{down,\xi}(x) = \frac{-\xi \det(\mathbf{H}) - \frac{\pi}{2} h_{22}}{h_{12}}. \quad (117)$$

From the above equation it is clear that for a fixed $x \in [0, h_{12} - h_{11}]$, $L_2^{down,\xi}(x)$ is a monotonically increasing function of $\xi \in [0, 1/2]$. Therefore for any $\xi \in [0, 1/2]$ we have

$$\begin{aligned} L_2^{down,\xi}(x) &\leq L_2^{down,1/2}(x) = L_2^{\xi=1/2}(x)/2, \quad \text{i.e.} \\ \min(L_2^{up,\xi}(x), L_2^{down,\xi}(x)) &\leq L_2^{\xi=1/2}(x)/2, \quad \text{i.e.} \\ 2 \min(L_2^{up,\xi}(x), L_2^{down,\xi}(x)) &\leq L_2^{\xi=1/2}(x), \quad \text{i.e.} \\ L_2^\xi(x) &\leq L_2^{\xi=1/2}(x). \end{aligned} \quad (118)$$

Therefore for case(b.I) finally we have

$$L_2^\xi(x) \leq L_2^{\xi=1/2}(x), \quad x \in [0, h_{12} - h_{11}]. \quad (119)$$

case (b.II) $x \in [h_{12} - h_{11}, L_1^{\max}(1/2)]$:

From (26) we have

$$\begin{aligned} \eta_3(\xi) &= 2\xi h_{12} - 2(1 - \xi)h_{11} \\ &= 2\xi(h_{12} + h_{11}) - 2h_{11} \end{aligned} \quad (120)$$

It is clear from the above equation that $\eta_3(\xi)$ is monotonically increasing with ξ and hence for $\xi \in [0, 1/2]$ we have

$$\begin{aligned} \eta_3(0) &\leq \eta_3(\xi) \leq \eta_3(1/2), \quad \text{i.e.} \\ -2h_{11} &\leq \eta_3(\xi) \leq h_{12} - h_{11}. \end{aligned}$$

Since $x \in [h_{12} - h_{11}, L_1^{\max}(1/2)]$ we have

$$\eta_3(\xi) \leq h_{12} - h_{11} \leq x, \quad \text{i.e.} \quad \eta_3(\xi) \leq x. \quad (121)$$

Therefore for case(b.II), from (25) and (26) we have

$$L_2^{up,\xi}(x) = \frac{-\xi \det(\mathbf{H}) - \frac{x}{2} h_{21}}{h_{11}}, \quad h_{12} - h_{11} \leq x \leq L_1^{\max}(1/2) \quad (122)$$

It is clear that $L_2^{up,\xi}(x)$ is monotonically increasing with ξ and hence using the similar argument as for (112) we can show that

$$L_2^\xi(x) \leq L_2^{\xi=1/2}(x). \quad (123)$$

Therefore using (119) and (123)¹⁷ for case (b) ($h_{12} \geq h_{11}$) we have

$$L_2^\xi(x) \leq L_2^{\xi=1/2}(x), \quad 0 \leq x \leq L_1^{\max}(1/2). \quad (124)$$

Therefore finally from (124) and (112) and Lemma 3 we have for any $\xi \in [0, 1]$

$$L_2^\xi(x) \leq L_2^{\xi=1/2}(x).$$

This completes the proof of Lemma 4. \blacksquare

Proof: Next using this Lemma we prove Theorem 1.

Towards this end, we consider an arbitrary $\xi \in [0, 1/2]$, for which we show that $R_{ZF}(\mathbf{H}, P_0/\sigma, \xi) \subseteq R_{ZF}(\mathbf{H}, P_0/\sigma, 1/2)$. For $\xi \in [1/2, 1]$, the proof is similar due to the symmetry of the $L_2^\xi(x)$ and $L_1^{\max}(\xi)$ functions (see Remark 1 and Lemma 3). For a given $\xi \in [0, 1/2]$ let $(R_1, R_2) \in R_{ZF}(\mathbf{H}, P_0/\sigma, \xi)$. From (14), we know that there exists a $Rect(L_1 \geq 0, L_2 \geq 0, D(\mathbf{H}, \xi)) \subset R_{//}(\mathbf{H})$ which corresponds to this rate pair (R_1, R_2) . Further from proposition 2, it follows that there exists

$$L_2^\xi(L_1) \geq L_2. \quad (125)$$

From Lemma (4) we know that for any a given $\xi \in [0, 1/2]$ and $0 \leq L_1 \leq L_1^{\max}(\xi)$, there exists

$$L_2^{\xi=1/2}(L_1) \geq L_2^\xi(L_1) \quad (126)$$

From (126) and (125) we get

$$L_2^{\xi=1/2}(L_1) \geq L_2. \quad (127)$$

We know that for $\xi = 1/2$ there exists a rectangle $Rect(L_1, L_2^{\xi=1/2}(L_1), D(\mathbf{H}, 1/2)) \subset R_{//}(\mathbf{H})$. From (127) it therefore follows that there will exist a rectangle $Rect(L_1, L_2, D(\mathbf{H}, 1/2)) \subset Rect(L_1, L_2^{\xi=1/2}(L_1), D(\mathbf{H}, 1/2))$ and hence $Rect(L_1, L_2, D(\mathbf{H}, 1/2)) \subset R_{//}(\mathbf{H})$. The rate pair corresponding to the rectangle $Rect(L_1, L_2, D(\mathbf{H}, 1/2))$ is (R_1, R_2) and therefore $(R_1, R_2) \in R_{ZF}(\mathbf{H}, P_0/\sigma, 1/2)$. \blacksquare

¹⁷In (119), $x \in [0, h_{12} - h_{11}]$, whereas in (123), $x \in [h_{12} - h_{11}, L_1^{\max}(1/2)]$, both of these cases we have the same result and for the union of both of these cases $x \in [0, L_1^{\max}(1/2)]$.

APPENDIX E PROOF OF THEOREM 2

Proof: The proof of Theorem 2 is as follows. Let $(a, \alpha a)$ be any arbitrary rate pair of the form $(r, \alpha r)$ lying strictly inside the rate region $R_{ZF}(\mathbf{H}, P_0/\sigma, \xi)$ and which does not lie on the boundary $R_{ZF}^{Bd}(\mathbf{H}, P_0/\sigma, \xi)$ (see the point P in Fig. ??).

We then show that there exists the unique rate pair $(a^*, \alpha a^*)$ which lies on the boundary $R_{ZF}^{Bd}(\mathbf{H}, P_0/\sigma, \xi)$ such that $a^* > a$. This shows that the rate pair $(R_{\max}^\alpha(\xi), \alpha R_{\max}^\alpha(\xi)) = (a^*, \alpha a^*)$ is the unique rate pair of the form $(r, \alpha r)$ which lies on the boundary.

Since, the rate pair $(a, \alpha a) \in R_{ZF}(\mathbf{H}, P_0/\sigma, \xi)$, from (14) such a pair $(a, \alpha a)$ will correspond to some rectangle $Rect(y, z > 0, D(\mathbf{H}, \xi))$ inside the parallelogram $R_{//}(\mathbf{H})$, where $0 \leq y < L_1^{\max}(\xi)$ such that

$$a = C(y, P_0/\sigma), \quad \text{and} \quad (128)$$

$$\alpha a = C(z, P_0/\sigma). \quad (129)$$

From (17), it follows that for the y given in (128), (i.e., for rate of User 1 given in (128)) the largest possible rate to the second user is given by

$$a_1 = C(L_2^\xi(y), P_0/\sigma). \quad (130)$$

From (18), it follows that the rate pair $(a, a_1) = (C(y, P_0/\sigma), C(L_2^\xi(y), P_0/\sigma))$ lies on the boundary $R_{ZF}^{Bd}(\mathbf{H}, P_0/\sigma, \xi)$. Since, a_1 is the largest possible rate of User 2 when rate of User 1 is equal to a (see the point Q in Fig. ??). it follows that

$$a_1 > \alpha a$$

$$C(L_2^\xi(y), P_0/\sigma) \stackrel{(a)}{>} C(z, P_0/\sigma), \quad \text{i.e.} \quad L_2^\xi(y) \stackrel{(b)}{>} z, \quad (131)$$

where step (a) follows from (130) and (129). Step (b) follows from the fact that $C(x, P_0/\sigma)$ is a monotonically increasing function of its first arguments. From the above equation it follows that z lies in the range of the function $L_2^\xi(x)$. It also follows from the continuity and monotonicity of $L_2^\xi(x)$ that there will exist a unique $0 \leq t \leq L_1^{\max}(\xi)$ such that

$$z = L_2^\xi(t) \quad (132)$$

From the last two equations it follows that

$$L_2^\xi(t) < L_2^\xi(y), \quad (133)$$

and hence since $L_2^\xi(x)$ is monotonically decreasing we have

$$y < t$$

$$C(y, P_0/\sigma) \stackrel{(a)}{<} C(t, P_0/\sigma), \quad \text{i.e.} \quad a \stackrel{(b)}{<} C(t, P_0/\sigma), \quad (134)$$

where step (a) follows from Result 2 and step (b) follows from (128). We have shown the rate pair $(C(t, P_0/\sigma), \alpha a)$ by the point R in Fig. 12.

We now define the function

$$f(x) \triangleq \alpha C(x, P_0/\sigma) - C(L_2^\xi(x), P_0/\sigma), \quad (135)$$

where $x \in [0, L_1^{\max}(\xi)]$. With increasing x , $C(x, P_0/\sigma)$ increases (see Result 2) and $C(L_2^\xi(x), P_0/\sigma)$ decreases (as

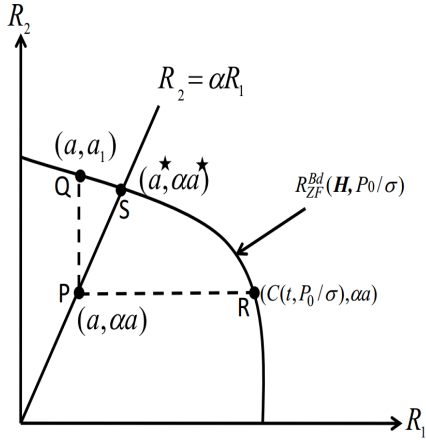


Fig. 12: A typical proposed rate region boundary.

$L_2^\xi(x)$ is a monotonically decreasing function of x , see Lemma 1). Hence $f(x)$ is a monotonically increasing function of x . Further, since $C(x, P_0/\sigma)$ and $L_2^\xi(x)$ are continuous functions, it follows that $f(x)$ is also continuous. It is clear that

$$f(y) \stackrel{(a)}{=} \alpha C(y, P_0/\sigma) - C(L_2^\xi(y), P_0/\sigma) \stackrel{(b)}{=} \alpha a - a_1 \stackrel{(c)}{<} 0, \quad (136)$$

where step (a) follows from (135), step (b) follows from (128) and (130), and step (c) follows from (131). Similarly

$$\begin{aligned} f(t) &\stackrel{(a)}{=} \alpha C(t, P_0/\sigma) - C(L_2^\xi(t), P_0/\sigma) \\ &\stackrel{(b)}{=} \alpha C(t, P_0/\sigma) - C(z, P_0/\sigma) \\ &\stackrel{(c)}{=} \alpha C(t, P_0/\sigma) - \alpha a \\ &= \alpha(C(t, P_0/\sigma) - a) \stackrel{(d)}{>} 0 \end{aligned} \quad (137)$$

where step (a) follows from (135), step (b) follows from the fact that $L_2^\xi(t) = z$ (see (132)). Step (c) follows from (129). Step (d) follows from (134).

Further, since $f(y) < 0$, $y \in [0, L_1^{\max}(\xi)]$ and $f(x)$, $x \in [0, L_1^{\max}(\xi)]$ is monotonically increasing in x , it follows that $f(x=0) < 0$. Similarly, $f(x=L_1^{\max}(\xi)) > 0$ since $f(t) > 0$ and $L_1^{\max}(\xi) \geq t$. Since, $f(x)$ is a monotonically increasing and continuous in $[0, L_1^{\max}(\xi)]$, and $f(0) < 0$, $f(t) > 0$, it follows that there exists a unique $x^* \in [0, L_1^{\max}(\xi)]$ such that $f(x^*) = 0$ [19]. The uniqueness follows from the monotonicity of $f(x)$. That is, from (135) we have

$$\alpha C(x^*, P_0/\sigma) = C(L_2^\xi(x^*), P_0/\sigma). \quad (138)$$

Let $a^* \triangleq C(x^*, P_0/\sigma)$ and therefore from (138) it follows that $\alpha a^* = C(L_2^\xi(x^*), P_0/\sigma)$. From (18), it is clear that the rate pair $(a^*, \alpha a^*) \in R_{ZF}^{Bd}(\mathbf{H}, P_0/\sigma, \xi)$. Uniqueness of such a rate pair follows from the uniqueness of x^* . Further since $f(y) < 0 = f(x^*)$ (see Eq. 136) and $f(x)$ is monotonically increasing, it follows that

$$x^* > y. \quad (139)$$

From Result (2) we know that $C(x, P_0/\sigma)$ is monotonically increasing in x and therefore from (139) $a^* = C(x^*, P_0/\sigma) > C(y, P_0/\sigma) = a$. Therefore we have shown that the unique

rate pair $(a^*, \alpha a^*)$ lies on the boundary $R_{ZF}^{Bd}(\mathbf{H}, P_0/\sigma, \xi)$ and $a^* > a$ for any arbitrary choice of a , where $(a, \alpha a)$ lies strictly inside $R_{ZF}(\mathbf{H}, P_0/\sigma, \xi)$. As shown in Fig. ??, the point $(a^*, \alpha a^*)$ lies on the line $R_2 = \alpha R_1$ and also on the boundary $R_{ZF}^{Bd}(\mathbf{H}, P_0/\sigma, \xi)$. This therefore completes the proof. ■

REFERENCES

- [1] H. Elgala, R. Mesleh, and H. Haas, "Indoor Optical Wireless Communication: Potential and State-of-the-Art," *IEEE Communications Magazine*, vol. 49, pp. 56–62, September 2011.
- [2] S. Dimitrov and H. Hass, *Principles of LED Light Communications: Towards Networked Li-Fi*. Cambridge University Press, 2015.
- [3] J. M. Kahn and J. R. Barry, "Wireless Infrared Communications," *Proceedings of the IEEE*, vol. 85, pp. 265–298, Feb 1997.
- [4] J. Y. Wang, J. B. Wang, M. Chen, and X. Song, "Dimming scheme analysis for pulse amplitude modulated visible light communications," in *2013 International Conference on Wireless Communications and Signal Processing*, pp. 1–6, Oct 2013.
- [5] J. B. Wang, Q. S. Hu, J. Wang, M. Chen, and J. Y. Wang, "Tight bounds on channel capacity for dimmable visible light communications," *Journal of Lightwave Technology*, vol. 31, pp. 3771–3779, Dec 2013.
- [6] A. Lapidoth, S. M. Moser, and M. A. Wigger, "On the Capacity of Free-Space Optical Intensity Channels," in *2008 IEEE International Symposium on Information Theory*, pp. 2419–2423, July 2008.
- [7] L. Wu, Z. Zhang, J. Dang, and H. Liu, "Capacity Lower Bounds of IM/DD AWGN Optical Wireless Channels Based on Fano's Inequality," in *Wireless Communications Signal Processing (WCSP), 2015 International Conference on*, pp. 1–5, Oct 2015.
- [8] A. Thangaraj, G. Kramer, and G. Bcherer, "Capacity Upper Bounds for Discrete-time Amplitude-Constrained AWGN Channels," in *2015 IEEE International Symposium on Information Theory (ISIT)*, pp. 2321–2325, June 2015.
- [9] J. G. Smith, "The Information Capacity of Amplitude and Variance Constrained Scalar Gaussian Channels," *Information and Control*, vol. 18, no. 3, p. 203–219, 1971.
- [10] A. A. Farid and S. Hranilovic, "Capacity of Optical Intensity Channels with Peak and Average Power Constraints," in *2009 IEEE International Conference on Communications*, pp. 1–5, June 2009.
- [11] J. B. Wang, Q. S. Hu, J. Wang, M. Chen, Y. H. Huang, and J. Y. Wang, "Capacity Analysis for Dimmable Visible Light Communications," in *2014 IEEE International Conference on Communications (ICC)*, pp. 3331–3335, June 2014.
- [12] T. Fath and H. Haas, "Performance Comparison of MIMO Techniques for Optical Wireless Communications in Indoor Environments," *IEEE Transactions on Communications*, vol. 61, pp. 733–742, Feb 2013.
- [13] T. V. Pham, H. L. Minh, Z. Ghassemlooy, T. Hayashi, and A. T. Pham, "Sum-Rate Maximization of Multi-User MIMO Visible Light Communications," in *2015 IEEE International Conference on Communication Workshop (ICCW)*, pp. 1344–1349, June 2015.
- [14] H. Shen, Y. Deng, W. Xu, and C. Zhao, "Rate-Maximized Zero-Forcing Beamforming for VLC Multiuser MISO Downlinks," *IEEE Photonics Journal*, vol. 8, pp. 1–13, Feb 2016.
- [15] A. Chaaban, Z. Rezki, and M. S. Alouini, "On the Capacity of the 2-User IM-DD Optical Broadcast Channel," in *2015 IEEE Globecom Workshops (GC Wkshps)*, pp. 1–6, Dec 2015.
- [16] A. Chaaban, Z. Rezki, and M. S. Alouini, "On the Capacity of the Intensity-Modulation Direct-Detection Optical Broadcast Channel," *IEEE Transactions on Wireless Communications*, vol. 15, pp. 3114–3130, May 2016.
- [17] T. Komine and M. Nakagawa, "Fundamental Analysis for Visible-Light Communication System Using LED Lights," *IEEE Transactions on Consumer Electronics*, vol. 50, pp. 100–107, Feb 2004.
- [18] B. Li, J. Wang, R. Zhang, H. Shen, C. Zhao, and L. Hanzo, "Multiuser MISO Transceiver Design for Indoor Downlink Visible Light Communication Under Per-LED Optical Power Constraints," *IEEE Photonics Journal*, vol. 7, pp. 1–15, Aug 2015.
- [19] W. Rudin, *Principles of Mathematical Analysis*. McGraw-Hill, 1976.